Elsevier Editorial System(tm) for Sensors & Actuators: B. Chemical

Manuscript Draft

Manuscript Number:

Title: N2S2 Pyridinophane-Based Fluorescent Chemosensors for Selective Optical Detection of Cd2+ in Soils

Article Type: Research Paper

Keywords: Macrocyclic ligands; Optical sensors; Fluorescent probes; Cadmium detection; Soil pollutants

Corresponding Author: Dr. Larisa Lvova, PhD

Corresponding Author's Institution: University Tor Vergata

First Author: Alessandra Garau

Order of Authors: Alessandra Garau; Larisa Lvova, PhD; Eleonora Macedi; Gianluca Ambrosi; M. Carla Aragoni; Massimiliano Arca; Claudia Caltagirone; Simon J. Coles; Mauro Formica; Vieri Fusi; Luca Giorgi; Francesco Isaia; Vito Lippolis; James B. Orton; Roberto Paolesse

Abstract: Herein we describe the synthesis and coordination properties in solution towards Zn2+ and Cd2+ of the ligands L1 and L2 containing the 2,8-dithia-5-aza-2,6-pyridinophane (L) macrocyclic receptor unit and the 2-(2′-hydroxy-3′-naphthyl)-4-methylbenzoxazole (HNBO) or 7-(2-ethylamino)-4-methylcoumarin chromophores. Spectrophotometric and spectrofluorimetric measurements in the UV-Visible region (MeCN/H2O solution 4:1 v/v) and 1H NMR measurements provided insight into the nature of complex species and transduction mechanisms responsible for the optical responses. The ligands showed an OFF-ON response upon addition of Zn2+ and Cd2+, for L1, and only Cd2+, for L2, in both cases attributable to the formation of 1:1 metal-to-ligand complexes. The crystal structure of [CdL2(NO3)2] is reported, being Cd2+ heptacoordinated by L and NO3- anions in a N2S2O3 environment. Exploiting the fluorescence properties of L1 and L2, an optical sensor array was developed featuring PVC membranes containing the dispersed sensing material and based on the Photoassisted Technique (PT) for signal acquisition, which allowed a quantitative determination of Cd2+ in real samples (soils). All phases from the design of the chemosensors to the development of the sensing device are discussed.

Suggested Reviewers: Luca Prodi
Full Professor, University of Bologna, Bologna, Italy
luca.prodi@unibo.it
Expert in chemosensors and fluorescent materials

Carlos Lodeiro Espino
Associate Professor, Faculdade de Ciencias e Tecnologia, Universidade Nova de Lisboa
cle@fct.unl.pt
Expert in chemosensors and fluorescent materials

Agata Michalska

Full Professor, Uniwersytet Warszawski
agatam@chem.uw.edu.pl
Expert in chemical sensors and sensor arrays

Enrique García-España
Full Professor, Instituto de Ciencia Molecular, Universitat de València
enrique.garcia-es@uv.es
Expert in chemosensors

Antonio Riul, Jr
University of Campinas, Brazil
iul@ufscar.br
Specialist in multisensory analysis

N_2S_2 Pyridinophane-Based Fluorescent Chemosensors for Selective Optical Detection of Cd^{2+} in Soils

Alessandra Garau,[a] Larisa Lvova,*[b] Eleonora Macedi,*[c] Gianluca Ambrosi,[c] M. Carla Aragoni,[a] Massimiliano Arca,[a] Claudia Caltagirone,[a] Simon J. Coles,[d] Mauro Formica,[c] Vieri Fusi,[c] Luca Giorgi,[c] Francesco Isaia,[a] Vito Lippolis,[a] James B. Orton [d] and Roberto Paolesse [c]*

[a]Dipartimento di Scienze Chimiche e Geologiche, Università degli Studi di Cagliari, S.S. 554 Bivio per Sestu, I-09042 Monserrato, Cagliari (Italy). E-mail: agarau@unica.it.

[b]Dipartimento di Scienze e Tecnologie Chimiche, Università di Roma "Tor Vergata", Via della Ricerca Scientifica 1, I-00133, Roma (Italy). E-mail: larisa.lvova@uniroma2.it.

[c]Dipartimento di Scienze Pure e Applicate, Università degli Studi di Urbino "Carlo Bo", via della Stazione 4, I-61029 Urbino (Italy). E-mail: eleonora.macedi@uniurb.it.

[d]UK National Crystallography Service, School of Chemistry, Faculty of Engineering and Physical Sciences, University of Southampton, SO17 1BJ, Southampton (United Kingdom).

Abstract. Herein we describe the synthesis and coordination properties in solution towards Zn^{2+} and Cd^{2+} of the ligands **L1** and **L2** containing the 2,8-dithia-5-aza-2,6-pyridinophane (**L**) macrocyclic receptor unit and the 2-(2′-hydroxy-3′-naphthyl)-4-methylbenzoxazole (HNBO) or 7-(2-ethylamino)-4-methylcoumarin chromophores. Spectrophotometric and spectrofluorimetric measurements in the UV-Visible region ($MeCN/H_2O$ solution 4:1 v/v) and ^1H NMR measurements provided insight into the nature of complex species and transduction mechanisms responsible for the optical responses. The ligands showed an OFF-ON response upon addition of Zn^{2+} and Cd^{2+}, for **L1**, and only Cd^{2+}, for **L2**, in both cases attributable to the formation of 1:1 metal-to-ligand complexes. The crystal structure of [Cd**L2**$(NO_3)_2$] is reported, being Cd^{2+} heptacoordinated by L and NO_3^- anions in a $N_2S_2O_3$ environment. Exploiting the fluorescence properties of **L1** and **L2**, an optical sensor array was developed featuring PVC membranes containing the dispersed sensing material and based on the Photoassisted Technique (PT) for signal acquisition, which allowed a quantitative determination of Cd^{2+} in real samples (soils). All phases from the design of the chemosensors to the development of the sensing device are discussed.

Keywords: cadmium detection; macrocyclic ligands; optical sensors; fluorescent probes; soil pollutants.

Introduction

The development of fluorescent molecular sensors for the recognition and sensing of heavy metal ions is a very important and active area of Supramolecular Chemistry having widespread applicative implications and due to their role as pollutants in soil, water and air [1-6]. Fluorescent chemosensors are among the best analytical tools for detecting and monitoring toxic heavy metal levels in environmental, industrial and biological samples because fluorescent measurements are sensitive, cheap, easy to be performed and the sample preparation is not disruptive offering the possibility of local observation through microscopy techniques.

In particular, the development of optical methodologies based on fluorescent chemosensors for the selective detection, discrimination and quantification of metal ions such as Zn^{2+} [4,7-13] and Cd^{2+} [4,13-21] has attracted increasing attention. In fact, both metal ions possess a closed-shell d^{10} configuration and, therefore, exhibit similar chemical properties, making their spectroscopic discrimination difficult. However, while Zn^{2+} is essential to life, Cd^{2+} is extremely toxic and carcinogenic [22]. Indeed, Zn^{2+} is the second most abundant transition metal in living organisms after iron and plays highly crucial roles in many biological processes, such as regulation of apoptosis, signal transmission, gene expression and enzyme function [23,24]. Unbalanced metabolism resulting from Zn^{2+} deficiency can be implicated in various neurological dysfunctions such as Alzheimer's disease [25], epilepsy and ischemic stroke [26]. Moreover Zn^{2+} becomes cytotoxic if assumed in large quantity, causing skin disease, diabetes, prostatic adenocarcinoma and pancreatic islets dysfunction [27]. In contrast, Cd^{2+} is a toxic metal ion for animals and human beings as it does not have a biological role in these species [22,28]. The mechanism of its toxicity is not understood clearly, but the effects on cells are known [29,30]. In human beings a high exposure to cadmium causes serious diseases such as renal dysfunctions and calcium metabolic disorders; moreover, it is classified as a human carcinogen and is associated with pulmonary, prostatic and renal cancer [22]. Due to the anthropogenic contamination the cadmium content in soils has grown significantly in the last decades [31]. The main sources of increasing cadmium content are the mining plants emissions, polluted sewage

sludges, as far as deposition from the atmosphere [32,33], where cadmium appears from industrial and vessel emissions, and waste incineration. From soil cadmium can easily enter the food-chain [34]. Thus, it is highly desirable to develop effective methods for monitoring Cd^{2+} and Zn^{2+} levels in biological, environmental and industrial matrices, based on novel fluorescent molecular sensors able to discriminate the two metal ions at least in terms of different optical response determined by their presence.

The most common fluorescent chemosensors consist of a fluorogenic fragment (signaling unit) covalently linked to a guest-binding site (receptor unit) *via* an appropriate spacer. An enhancement or quenching of the fluorescence emission of the signaling unit generally accompanies the host-guest interaction of the target species with the receptor unit, following the perturbation of a variety of photo-induced electronic processes [35-37].

The critical point in this "receptor-spacer-fluorophore" supramolecular modular synthetic scheme is the accurate choice of both the signaling and the receptor units, particularly if a direct interaction between the fluorophore and the target species is possible, in order to achieve thermodynamic/optical selectivity of the sensor and high sensitivity or chemosensor performance [35]. In principle, the thermodynamic selectivity of a fluorescent chemosensor not necessarily entails its optical selectivity and vice-versa. However, an optical response selectivity shown by a chemosensor still represents a favorable situation for analytical applications, since analytes interfering in the binding process might not be present in the analyzed matrices, or only a qualitative response of the target species may be required. Furthermore, it is possible to gain also the binding selectivity for a chemosensor showing only the optical one by testing different media for the host-guest interaction (solutions, membranes, hard and soft nanoparticles), where other factors (lipophilicity of the chemosensor and its complexes, and their mobility) governing transport processes can strongly influence the binding affinity of the fluorescence chemosensors in a way to reach also the thermodynamic selectivity [35].

Based on these considerations, to easily achieve fluorescent chemosensors showing at least the optical selectivity for a given target metal ion, in the last decade we have adopted the synthetic strategy (we called "complementary") of

considering a predefined receptor unit and attaching to it in turn different fluorogenic fragments counting on a "synergic cooperation" between the two units of the resulting conjugated chemosensors in determining at least the optical selectivity.

Among others, we have focused our attention on the macrocycle 2,8-dithia-5-aza-2,6-pyridinophane (**L**) as a receptor unit, which forms stable 1:1 complexes with a variety of metal ions, and we have covalently linked to it different fluorogenic fragments as reported in Fig. 1, obtaining a different optical selectivity depending on the signaling unit and the experimental conditions used [38-45].

<Insert Figure 1>

It is important to underline that no metal-selective change in the fluorescence emission of $\mathbf{L_A}$ is observed in agreement with the fact that the anthracenyl moiety does not participate to the complexation process of the metal ion [38]. Using $\mathbf{L_D}$, an efficient new flow-injection analysis (FIA) system based on liquid–liquid microextraction method for the on-line separation, pre-concentration and fluorimetric determination of Zn^{2+} was developed with a detection limit of 2.4 ng/mL [41]. In the designed FIA system, by using *n*-hexanol as extracting organic solvent and choosing the appropriate experimental conditions, the extraction of $\mathbf{L_D}$-coordinated Zn^{2+} becomes extremely selective also with respect to Cd^{2+}, the only interfering metal in the optical response of $\mathbf{L_D}$ towards Zn^{2+}. On the other hand, $\mathbf{L_E}$ has been used to detect Cd^{2+} in cells in vitro and in living cells by flow cytometry, being the fluorescence directly correlated with Cd^{2+} content in cells [39]. Finally, $\mathbf{L_F}$ and $\mathbf{L_G}$ have been used in water, to measure Hg^{2+} and Pd^{2+} levels [43,44], respectively, once loaded on silica core–polyethylene glycol (PEG) shell nanoparticles or supported on polyvinyl chloride (PVC) membranes ($\mathbf{L_F}$) in combination with familiar Photoassisted Technique (PT).

Following our interest in developing fluorescent chemosensors able to perform a Zn^{2+}/Cd^{2+} optical discrimination for possible analytical applications [45,46], herein we describe the synthesis and recognition/sensing properties in solution towards metal ions of the two ligands **L1** and **L2** containing the 2-(2'-

hydroxy-3'-naphthyl)-4-methylbenzoxazole (HNBO) and the 7-(2-ethylamino)-4-methylcoumarin chromophores, respectively, as pendant arms (Fig. 2).

<Insert Figure 2>

These ligands have been used previously for the construction of an optical sensor array for the recognition of Cd^{2+} and NO_2^- ions in water samples [47]. Herein, their suitability once implemented with familiar devices for signal acquisition (Light Emitting Diode, LED, as light source, and a digital camera as a signal detector), and chemometric methods for data treatment to perform fast and low-cost monitoring of Cd^{2+}, in soil samples, is also demonstrated.

Experimental

Instruments and materials

Microanalytical data were obtained using a Thermo Finnigan Flash 1112 EA CHN analyzer (**L1**) and a Fisons EA CHNS-O instrument (T = 1000 °C, **L2**). Mass spectra were acquired with a HPLC system (Waters Alliance 2795) coupled with a photodiode array detector (Waters 2996 PDA), followed by an electrospray mass spectrometer detector (ESI-MS) (Waters-Micromass ZQ) worked by Mass Lynx 4.1 SP4 software (**L1**) and with a triple quadruple QqQ Varian 310-MS mass spectrometer using the Atmospheric-Pressure Electrospray Ionization technique worked by mMass 5.5.0 software package (**L2**). Polyvinyl chloride (PVC) high molecular weight, tris(2-ethylhexyl)phosphate (TOP), bis(2-ethylhexyl)sebacate (DOS), o-nitrophenyl octyl ether (o-NPOE), potassium tetrakis-(4-chlorophenyl)borate (TpClPBK), tetrahydrofuran (THF), 2-(N-morpholino)ethanesulfonic acid (MES), 4-(2-hydroxyethyl)piperazine-1-ethane-sulfonic acid (HEPES), tris(hydroxymethyl)aminomethane (TRIS) and 3-(N-morpholino)propanesulfonic acid (MOPS) were purchased from Sigma-Aldrich. 2,8-dithia-5-aza-2,6-pyridinophane (**L**) [38] and 7-[(2-Bromoethyl)amino]-4-methylcoumarin [48] were prepared by published methods. THF was freshly distilled prior to use. All the other chemicals and solvents were of analytical grade and used without further purification. For spectrophotometer measurements, MeCN (Uvasol, Merck) and Millipore grade water were used as solvents.

UV–Vis and fluorescence emission experiments

The spectrophotometric measurements were carried out at 298.1 K using a Varian Cary-100 spectrophotometer equipped with a temperature control unit (**L1**) and a Thermo Nicolet Evolution 300 spectrophotometer (**L2**). Uncorrected emission spectra were obtained with a Varian Cary Eclipse fluorescence spectrophotometer. Luminescence quantum yields were determined using 2,2'-biphenol in acetonitrile (Φ = 0.29)[49] and quinine sulphate in a 1 M H_2SO_4 aqueous solution (Φ = 0.546) as references for **L1** and **L2**, respectively.

All UV–Vis and fluorescence emission measurements were performed in MeCN/H_2O (4:1 v/v) at pH 7.4 (MOPS buffer $1.0 \cdot 10^{-2}$ M) at 25 °C. Screenings with various metal ions were carried out by adding 1 equiv. of M^{n+} (M^{n+} = Cd^{2+}, Co^{2+}, Cu^{2+}, Fe^{3+}, Hg^{2+}, K^{+}, Mg^{2+}, Al^{3+}, Ni^{2+}, Zn^{2+} and Pb^{2+}) as their nitrate, chloride or perchlorate to a solution of **L1** and **L2** (**L1** = $5.0 \cdot 10^{-6}$ M, **L2** = $2.5 \cdot 10^{-5}$ M). All samples were stored and measured again after 6, 24, 48, 96 h. Spectrofluorimetric titrations of **L1** and **L2** with metal ions were performed by adding to a solution of the ligand (3 mL), buffered at pH 7.4 with MOPS increasing volumes of a solution of the metal ions and keeping the solution mixed for 5 min before starting the acquisition of each spectrum.

Ion competition studies were performed either by adding 1 equiv. of Zn^{2+} or Cd^{2+} to an equimolar solution of **L1** or **L2** and M^{n+}, or by adding 5 equivs. of M^{n+} to an equimolar solution of **L1** and Zn^{2+} or **L2** and Cd^{2+} (**L1** = $5.0 \cdot 10^{-6}$ M, **L2** = $2.5 \cdot 10^{-5}$ M, M^{n+} = Cd^{2+}, Co^{2+}, Cu^{2+}, Fe^{3+}, Hg^{2+}, K^{+}, Mg^{2+}, Al^{3+}, Ni^{2+} and Pb^{2+}). All samples were stored and measured again after 5, 24, 48 and 120 h.

NMR experiments

^{1}H and ^{13}C NMR spectra were recorded on a Bruker Avance 400 instrument, operating at 400.13 and 100.61 MHz, respectively, and equipped with a variable temperature controller. The temperature of the NMR probe was calibrated using 1,2-ethanediol as a calibration sample (**L1**). In the case of **L2**, ^{1}H and ^{13}C NMR spectra were recorded on a Varian VXR500 and on a Bruker Avance III HD 600 MHz spectrometer, and peak positions are reported relative to tetramethylsilane ($SiMe_4$). For the spectra recorded in $CDCl_3$, CD_3CN and DMSO-d_6 the ^{1}H and ^{13}C peak positions are reported with respect to the residual solvent. Chemical shifts (δ scale) are reported in parts per million (ppm) and coupling

constants (*J*) are given in Hertz (Hz). $^{1}H–^{1}H$ and $^{1}H–^{13}C$ correlation experiments were performed to assign the signals.

All NMR measurements were carried out in DMSO-d_6 for **L1** and in CD_3CN/CD_3Cl (7:3 v/v) for **L2**. In the case of **L1**, Zn^{2+} and Cd^{2+} ions were added as perchlorate salts while in the case of **L2**, Cd^{2+} ion was added as nitrate salt. NMR spectra of protonated and deprotonated forms of **L1** were acquired in DMSO-d_6 after the addition to a $1.0 \cdot 10^{-2}$ M solution of the ligand of, respectively, 1 drop of DCl and 1 equiv. of Bu_4NOH.

In a typical experiment, to a solution of the ligand (**L1**-**L2** = $1.0 \cdot 10^{-2}$ M) was added the metal ion directly in the NMR tube, that was then kept for 10 min at a temperature of 298.1 K before starting the acquisition of the spectrum. The same procedure was followed for the addition of 1 equiv. of Bu_4NOH (0.1 M solution) to the pre-formed **L1**-metal solution.

X-ray crystallography

A summary of the crystal data and refinement details for the compound [Cd**L2**$(NO_3)_2$] (**1**) discussed in this paper is presented in Table S4 (ESI). The sample was suspended in perfluoroether oil; a suitable pale yellow lath-shaped single crystal of size 0.150 × 0.090 × 0.010 mm^3 was selected and mounted on a MiTeGen holder with perfluoroether oil, then aligned upon a Rigaku FRE+ diffractometer, equipped with VHF Varimax confocal mirrors, a Rigaku AFC12 goniometer and an enhanced sensitivity (HG) Saturn724+ CCD detector equipped with an Oxford Cryosystems low-temperature device. The crystal was kept at a steady T = 100(2) K during data collection. The structure was solved with the ShelXT [50] solution program using dual methods and by using Olex2 [51] as the graphical interface. The model was refined with ShelXL 2018/3 [52] using full matrix least squares minimization on F^2.

Optodes preparation and testing

Membranes contained from 1-3 wt % of fluorophore, 2-8 wt % of TpClPBK in PVC/plasticizer polymeric matrix in ratio 1:2 by weight. All components were dissolved in freshly distilled THF, and 5-7 μL of this membrane cocktail were cast onto transparent glass slide support. For every membrane 2-4 spots were deposited on the same support to guarantee the replicated measurements. Where

required, up to 10 sensing spots from membrane cocktails of different composition were deposited in total on the same glass support, thus providing an optical sensors array. The THF solvent was allowed to evaporate overnight to form all-solid-state optodes with polymeric membrane films adhesive to the glass slide surface.

Due to fluorophores photosensitivity, freshly prepared "disposable" sensors were employed, in order to avoid photodegradation problems; the membranes were deposited onto transducer surfaces few hours prior to measurement. Membranes were kept in the dark before use. The membrane responses towards primary Cd^{2+}, Zn^{2+} ions in their individual and binary solutions, as far as towards Li^{+}, Na^{+}, K^{+}, NH_4^{+}, Ca^{2+}, Mg^{2+}, Cu^{2+}, Co^{2+} and Pb^{2+} as potential interfering ions were tested in concentration range from $3.3 \cdot 10^{-7}$ to $2.2 \cdot 10^{-2}$ M. 1 M stock solutions of metal salts were prepared dissolving corresponding amounts of metal chlorides and Pb^{2+} and Zn^{2+} nitrates in distilled water, solutions of lower concentrations were obtained by consecutive additions of calculated amounts of corresponding stock solution in 0.01 M background of (MES pH 5.5, HEPES pH 7.5, or TRIS pH 8.6).

Optodes luminescence was measured with a photometric setup, performed in polystyrene cuvettes (Katrell, model 1937) of 10 mm path length using a Photoassisted Technique (PT) measurement setup.[47] A blue-colored InGaN LED (Roithner LaserTechnik, Austria, model H2A1-H385, λ_{ex} = 380 nm) was employed as monochromic external light source. The transparent cuvette was laterally illuminated with LED and the response of optode upon analyte addition was registered with respect to the tree main visible spectrum colors: Red (630 nm), Green (530 nm), and Blue (480 nm). The sensing spot RGB signals, and the luminescence intensity, I, evaluated as the mean value of RGB response were evaluated after background luminosity subtraction. The overall measurement duration was 60 s, during this period the defined areas (of 5 px diameter) of optode sensing membrane were chosen for further digital signal extraction from these zones (mask selection step), followed by 10 consecutive snapshots taken every 5 s, and the final optical signal was a mean value of these records. The measurement chamber was properly shielded from ambient illumination. The responses of optical sensors were registered and digitalized in analytically useful

signals by in house written MATLAB (v.7.0, 2005, The MathWorks, Inc., Natick, USA) codes.

Real Samples analyses

Developed optical sensors were tested both in a single sensor mode and inside the sensor array for assessment of Cd^{2+} spiked in aqueous extracts of three soil samples: the first one was sampled close to the landing strip of one of the Rome airports (Ciampino G.B. Pastine airport, Italy), another sample was delivered from illegal waste dump from Naples zone (Castello di Cisterna, NA, Italy), the last soil was sampled from "Tor Vergata" University garden of Faculty of Science (Sogene building, Tor Vergata zone of Rome, Italy). The raw soil samples of approximately 50 g weight were handpicked from the surface of 0.5 m^2 in selected sites, mixed and sieved, afterwards 1 g amount of every sample was weighted inside glass vessel and extracted with 5 mL in 0.01 M HEPES pH 7.5 solution for 24 h. The filtrate was then separated from solid soil precipitate, placed in transparent cuvette and tested with developed optical sensors for Cd^{2+} content without any other pre-treatment. The standard addition method was employed, for this the additions of $1.0 \cdot 10^{-5}$ M and $1.1 \cdot 10^{-4}$ M of Cd^{2+} ions were performed to 2 mL of filtrate and the luminescence variance of the sensors was registered with the PT technique.

The amount of Cd^{2+} ions in analyzed soil samples was evaluated by standard Atomic Absorption Spectroscopy (AAS) method on Perkin Elmer AAnalyst 600 high performance optical system combined with a Transversely Heated Graphite Atomizer (THGA) furnace assembly. AAS was calibrated with standard solutions contained 1 mg/mL of Cd^{2+} (Carlo Erba, Italy) by 3 points calibration. The 228.8 nm wavelength was employed for Cd^{2+} optical detection.

The Partial Least Squares (PLS) regression method was applied to interpret the optical output of the sensor array composed of **L1**- and **L2**-based membranes Mb6 and Mb12 and employed for analysis of the Cd^{2+} content in soils. PLS was used to correlate the optode array output (Y-variable) with the known concentrations of Cd^{2+} (X-variables) in 7 calibration solutions measured in triplicate on two sensing spots of the same membrane (n = 6) and test solutions extracted from soils. Data treatment was performed with commercial Unscrambler (v. 9.1, 2004, CAMO PROCESS AS, Norway). Due to the restricted

number of analyzed samples the validation was performed by using a leave-one-out cross-validation procedure. The RMSEC and RMSEV (Root Mean Square Error of Calibration and Validation, respectively) and the correlation coefficients, R^2, of predicted *versus* measured correlation lines were used to evaluate the efficiency of the applied regression model.

Synthesis

2-(2'-Hydroxy-3'-naphthyl)-4-methylbenzoxazole (HNBO, 3). Polyphosphoric acid (40 g) was heated to dissolution, then 3-hydroxy-2-naphthoic acid (**1**, 7.5 g, 40 mmol) and 2-amino-*m*-cresol (**2**, 4.9 g, 40 mmol) were added to the solution and the mixture was stirred at 160 °C for 16 h. The reaction mixture was cooled to room temperature and poured into ice-water to stop the reaction, then the suspension was neutralized with Na_2CO_3 and the solid obtained was collected by filtration and washed with water. The crude product was purified by Soxhlet extraction and recrystallization from n-hexane, to obtain a yellow solid (7.0 g, 25 mmol, 64% yield). ^{1}H NMR (400 MHz, $CDCl_3$): δ = 2.68 (s, 3H), 7.22 (d, J = 6.8 Hz, 1H), 7.33 (t, J = 8.0 Hz, 1H), 7.37 (t, J = 7.6 Hz, 1H), 7.47 (s, 1H), 7.50 (m, 2H), 7.75 (d, J = 8.0 Hz, 1H), 7.89 (d, J = 8.0 Hz, 1H), 8.64 (s, 1H) ppm. ^{13}C NMR (100 MHz, $CDCl_3$): δ = 16.49, 107.94, 111.54, 112.79, 123.98, 125.55, 125.65, 126.47, 127.48, 128.34, 128.42, 128.66, 130.14, 136.60, 139.36, 149.04, 154.22, 161.77 ppm. Anal. Calcd (%) for $C_{18}H_{13}NO_2$: C, 78.53; H, 4.76; N, 5.09. Found: C, 78.4; H, 4.8; N, 5.0.

2-(2'-Methoxymethyloxy-3'-naphthyl)-4-methylbenzoxazole (4). HNBO (**3**) (7.0 g, 25 mmol) was dissolved in anhydrous CH_2Cl_2 (50 mL), then N,N-diisopropylethylamine was added (24.0 g, 190 mmol). The mixture was cooled to 0 °C, then a solution of chloromethyl methyl ether (MOMCl, 15.0 g, 190 mmol) in anhydrous CH_2Cl_2 (20 mL) was slowly added and the reaction mixture was refluxed overnight. Water was poured into the solution and the product was recovered by extraction and successively washed twice with water. The extracted organic layer was dried over anhydrous Na_2SO_4 and evaporated to afford the crude product. Silica gel column purification with CH_2Cl_2/n-hexane (1:1, v/v)

afforded the final product **4** as a light pink solid (7.0 g, 22 mol, 88% yield). ^{1}H NMR (400 MHz, DMSO-d_6): δ = 2.64 (s, 3H), 3.53 (s, 3H), 5.46 (s, 2H), 7.26 (td, ^{3}J = 7.6 Hz, ^{4}J = 0.8 Hz, 1H), 7.35 (t, J = 7.6 Hz, 1H), 7.50 (td, ^{3}J = 7.6 Hz, ^{4}J = 1.2 Hz, 1H), 7.60 (m, 2H), 7.71 (s, 1H), 7.92 (d, J = 7.6 Hz, 1H), 8.08 (d, J = 7.6 Hz, 1H), 8.66 (s, 1H) ppm. ^{13}C NMR (100 MHz, DMSO-d_6): δ = 16.69, 56.52, 95.34, 108.58, 111.78, 118.74, 125.51, 125.55, 125.68, 127.18, 128.60, 128.86, 129.00, 130.41, 132.55, 135.61, 141.04, 150.61, 152.52, 160.95 ppm. Anal. Calcd (%) for $C_{20}H_{17}NO_3$: C, 75.22; H, 5.37; N, 4.39. Found: C, 75.2; H, 5.5; N, 4.3.

4-Bromomethyl-2-(2'-methoxymethyloxy-3'-naphthyl)-benzoxazole (5). A CCl_4 solution (100 mL) of **4** (3.0 g, 9.4 mmol), N-bromosuccinimide (NBS, 1.8 g, 10.4 mmol) and azobisisobutyronitrile (AIBN, 0.75 g, 4.6 mmol) was refluxed overnight under nitrogen atmosphere. The obtained suspension was cooled and filtered, then the filtrate was evaporated under vacuum. Silica gel column purification with CH_2Cl_2/n-hexane (1:1, v/v) afforded the final product as a white powder (2.3 g, 5.8 mmol, 62% yield). ^{1}H NMR (400 MHz, $CDCl_3$): δ = 3.64 (s, 3H), 5.01 (s, 2H), 5.47 (s, 2H), 7.37 (t, J = 8.7 Hz, 1H), 7.93 (d, J = 8.2 Hz, 1H), 7.45 (m, 2H), 7.57 (m, 3H), 7.80 (d, J = 8.2 Hz, 1H), 8.68 (s, 1H) ppm. ^{13}C NMR (100 MHz, $CDCl_3$): δ = 27.83, 56.57, 95.44, 110.74, 111.77, 118.40, 125.07, 125.11, 125.25, 126.89, 128.29, 128.61, 128.73, 129.74, 132.78, 135.68, 140.72, 150.89, 152.69, 162.06 ppm.

5-(2-(2'-Methoxymethyloxy-3'-naphthyl)-benzoxazol-4-ylmethyl)-2,8-dithia-5-aza-2,6-pyridinophane (6). Na_2CO_3 (670 mg, 6.30 mmol) was added to an anhydrous DMF (20 mL) suspension of 2,8-dithia-5-aza-2,6-pyridinophane (**L**)[38] under nitrogen atmosphere. The reaction mixture was heated at 50 °C, then an anhydrous DMF (20 mL) solution of **5** (250 mg, 0.630 mmol) was added dropwise under nitrogen. The mixture was reacted at 50 °C for 3 days, then the desired product was isolated by precipitation following addition of ice and water (50 mL). The obtained solid was filtered off, dissolved in CH_2Cl_2 and dried over anhydrous Na_2SO_4. Following solvent evaporation, the crude product was purified by chromatography on alumina column eluting with CH_2Cl_2 to afford **7** as a white solid (120 mg, 0.22 mmol, 38% yield). ^{1}H NMR (400 MHz, DMSO-d_6): δ = 2.58 (m, 8H), 3.51 (s, 3H), 3.83 (s, 4H), 4.03 (s, 2H), 7.40 (m, 4H), 7.50 (td, ^{3}J = 7.6 Hz, ^{4}J = 1.1 Hz, 1H), 7.61 (td, ^{3}J = 7.6 Hz, ^{4}J = 1.1 Hz, 1H), 7.66 (dd, ^{3}J = 6.8 Hz, ^{4}J =

1.6 Hz, 1H), 7.71 (s, 1H), 7.83 (t, J = 8.0 Hz, 1H), 7.91 (d, J = 8.0 Hz, 1H), 8.06 (d, J = 8.0 Hz, 1H), 8.63 (s, 1H) ppm. ^{13}C NMR (100 MHz, DMSO-d_6): δ = 25.32, 36.05, 51.62, 52.82, 109.43, 111.23, 112.74, 121.71, 124.30, 124.86, 125.10, 126.15, 126.43, 127.66, 128.81, 128.95, 129.00, 131.90, 136.80, 138.54, 138.87, 149.31, 154.18, 158.01 ppm. Anal. Calcd (%) for $C_{31}H_{31}N_3O_3S_2$: C, 66.76; H, 5.60; N, 7.53. Found: C, 66.8; H, 5.7; N, 7.4.

5-(2-(2'-Hydroxy-3'-naphthyl)-benzoxazol-4-ylmethyl)-2,8-dithia-5-aza 2,6-pyridinophane (L1). *p*-Toluenesulfonic acid (TsOH, 210 mg, 1.10 mmol) was added in one portion to a stirred anhydrous methanolic solution (10 mL) of **6** (60 mg, 0.11 mmol) under nitrogen atmosphere. The mixture was reacted at room temperature for 3 days, then the solvent was evaporated under vacuum. The residue was dissolved in CH_2Cl_2 (15 mL) and washed twice with a saturated solution of $NaHCO_3$ (10 mL). The extracted organic layer was dried over anhydrous Na_2SO_4, filtered off and evaporated to afford the final product as a yellow solid (50 mg, 0.10 mmol, 90% yield). ^{1}H NMR (400 MHz, DMSO-d_6): δ = 2.57 (m, 8H), 3.83 (s, 4H), 4.02 (s, 2H), 7.37 (d, J = 7.6 Hz, 2H), 7.42 (m, 2H), 7.46 (t, J = 7.6 Hz, 1H), 7.50 (s, 1H), 7.56 (td, ^3J = 7.6 Hz, ^4J = 1.2 Hz, 1H), 7.74 (dd, ^3J = 7.6 Hz, ^4J = 1.2 Hz, 1H), 7.82 (d, J = 7.6 Hz, 1H), 7.84 (t, J = 8.0 Hz, 1H), 8.06 (d, J = 8.0 Hz, 1H), 8.73 (s, 1H), 11.10 (s, 1H) ppm. ^{13}C NMR (100 MHz, DMSO-d_6): δ = 25.47, 36.10, 51.63, 52.86, 109.83, 111.54, 113.22, 122.05, 124.63, 125.27, 126.38, 126.64, 127.60, 129.14, 129.30, 129.60, 131.81, 136.59, 138.93, 139.03, 149.35, 153.87, 157.95, 162.01 ppm. MS (ESI): m/z = 514.1 $[M-H]^+$. Anal. Calcd (%) for $C_{29}H_{27}N_3O_2S_2$: C, 67.81; H, 5.30; N, 8.18. Found: C, 67.9; H, 5.6; N, 8.0.

7-[2-ethylamino]-4-methylcoumarin-2,8-dithia-5-aza-2,6-pyridinophane (L2). To a mixture of 2,8-dithia-5-aza-2,6-pyridinophane, **L** [38] (0.20 g, 0.83 mmol), K_2CO_3 (0.180 g, 1.66 mmol) and NaI (0.12 mL, 0.83 mmol) was added 7-[(2-Bromoethyl)amino]-4-methylcoumarin (0.23 g, 0.83 mmol) in anhydrous acetonitrile (20 mL). The reaction mixture was heated at 80 °C for 48 hours under nitrogen and 24 hours at room temperature. The solid was filtered off, and the solvent was removed under reduced pressure. The residue was dissolved in CH_2Cl_2 and washed with water. The organic phase was dried over Na_2SO_4, and the solvent removed under reduced pressure to give a yellow solid (0.10 g, 27% yield). ^{1}H NMR (500 MHz, $CDCl_3$): δ = 2.33 (s, 3H), 2.56 (m, 8H), 2.70 (t, J = 9.8 Hz,

2H), 3.05 (m, 2H), 3.83 (s, 4H), 4.93 (bs, 1H), 5.96 (s, 1H), 6.37 (m, 1H), 6.46 (m, 1H), 7.31 (m, 3H), 7.72 (t, J = 12.8 Hz, 1H). ^{13}C NMR (150.9 MHz, $CDCl_3$): δ = 18.53, 26.37, 36.72, 40.41, 47.19, 51.23, 51.75, 98.33, 109.34, 110.51, 110.59, 121.63, 125.40, 138.32, 151.61, 152.95, 155.96, 157.92, 162.03 ppm. MS (ESI): m/z = 442 $[M-H]^+$. Anal. Calcd (%) for $C_{23}H_{27}N_3O_2S_2$: C, 62.6; H, 6.2; N, 9.5. Found: C, 61.9; H, 5.9; N, 9.9.

[CdL2(NO$_3$)$_2$] (1). $Cd(NO_3)_2 \cdot 4H_2O$ (7.0 mg, 0.0027 mmol) in MeCN (1 mL) was added to a solution of **L2** (10.0 mg, 0.00270 mmol) in MeCN/CH_2Cl_2 (5 mL, 4:1 v/v). The solution was stirred at room temperature for 24 hours. The yellow solid obtained was dissolved in DMF and pale yellow crystals were obtained by diffusion of Et_2O vapors in the solution (50% yield). Anal. Calcd (%) for $C_{23}H_{27}N_5O_8S_2Cd$: C, 40.7; H, 4.0; N, 10.3. Found: C, 40.2; H, 3.8; N, 9.8.

Results and discussion

Synthesis of L1 and L2

L1 was synthesized adapting the five steps procedure already described by Kwon *et al* . [53] (Scheme 1). The acid-catalyzed condensation between 2-amino-*m*-cresol (**2**) and 2-hydroxy-3-naphthoic acid (**1**) gave the fluorophore **3** (HNBO), which was sequentially protected on the naphthol group by conversion to methoxymethyl acetal (MOM) (**4**) and activated by bromination with N-bromosuccinimide (NBS) and azobisisobutyronitrile (AIBN) on the methyl group to afford the bromomethyl derivative **5**. The reaction between the bromide **5** and **L**, whose synthesis was previously described [38], affords the MOM-protected compound **6**. The MOM group was finally removed by *p*-toluenesulfonic acid (TsOH) to yield **L1**.

L2 was synthesized by reacting 7-[(2-bromoethyl)amino]-4-methyl coumarin with **L** in acetonitrile in the presence of K_2CO_3.

<Insert Scheme 1>

Metal complexation by L1

In order to explore the properties of the two ligands as fluorescent chemosensors for metal ions recognition, a spectrophotometric and spectrofluorimetric screening of the sensing ability of **L1** and **L2** towards several

metal ions was performed, namely Cd^{2+}, Co^{2+}, Cu^{2+}, Fe^{3+}, Hg^{2+}, K^{+}, Mg^{2+}, Al^{3+}, Ni^{2+}, Zn^{2+} and Pb^{2+} (as nitrate, chloride or perchlorate salts). The absorption spectrum of **L1** in MeCN/H_2O (4:1 v/v) (Kw: $4.47 \cdot 10^{-18}$) [54] at pH = 7.4 (MOPS buffer, $1.0 \cdot 10^{-2}$ M) mainly shows two intense bands at 331 (ε = 38600 $mol^{-1}dm^3cm^{-1}$) and 318 nm (ε = 47000 $mol^{-1}dm^3cm^{-1}$) and a shoulder centered at 370 nm (ε = 6600 $mol^{-1}dm^3cm^{-1}$) (black line in Fig. S1, ESI).

The addition of Zn^{2+}, Cd^{2+}, Ni^{2+}, Cu^{2+}, Co^{2+} and Hg^{2+} ions significantly modifies the absorption spectrum of **L1** (Fig. S1a, ESI). In particular, a new band centered at 434 nm (Cd^{2+}, Co^{2+} and Hg^{2+}), 438 nm (Zn^{2+}), 442 nm (Ni^{2+}) or 444 nm (Cu^{2+}) grew upon the addition of the metal cation, turning the solution from colorless to yellow. At the same time, the shoulder at 370 nm disappeared, the band at 318 nm decreased, while two new bands at 346 and 288 nm arose. To a lesser extent, Pb^{2+}, K^{+}, Mg^{2+} and Fe^{3+} ions induce similar changes in the absorption spectrum of **L1** (Fig. S1b, ESI). Noteworthy, only Zn^{2+}, Cd^{2+}, Cu^{2+}, Co^{2+} and Hg^{2+} ions affect the absorption spectrum of **L1** immediately upon their addition, the remaining metal ions require instead a longer time (one day). Under these experimental conditions, only Al^{3+} does not perturb the absorption spectrum of **L1** at all.

In the HNBO fluorogenic unit of **L1** an intramolecular hydrogen bond can form between the -OH group and the proton-withdrawing N-atom of the oxazole moiety in a six-membered ring. In such system, tautomerization occurs following photoexcitation, transiently producing a keto-form whose fluorescence emission is bathochromically shifted with respect to the enol-form, which in turn forms when the excited-state intramolecular proton transfer (ESIPT) process is suppressed by metal coordination [37].

Accordingly, **L1** exhibits a peculiar triple emission fluorescence spectrum, with three bands at 417, 558 and 630 nm (λ_{ex} = 320 nm, Φ = 0.010; dashed line in Fig. S2, ESI). The former and the latter bands are related to the fluorescence of the enol- and keto-form of the ligand, respectively [53]; the emission intensity of the keto-form is very weak, so is the band that occurs at 558 nm, that, as will be discussed in the following, is ascribable to the deprotonated form of the ligand. This last band undergoes a remarkable and immediate intensity enhancement upon addition of 1 equiv. of Zn^{2+} and Cd^{2+} at pH = 7.4 (Fig. 3). Moreover, a weaker

emission enhancement occurs in the presence of 1 equiv. of Fe^{3+}, Hg^{2+}, Ni^{2+}, Pb^{2+}, K^{+} and Mg^{2+}, but on a longer time scale (one to two days) (Fig. 3).

<Insert Figure 3>

Due to the remarkable CHEF effect observed for **L1** in the presence of Zn^{2+} and Cd^{2+} ions, the binding properties of the ligand towards these two cations have been further investigated by performing UV-Vis and fluorescence (λ_{ex} = 320 nm) spectrophotometric titrations of **L1** with Zn^{2+} and Cd^{2+} ions in MeCN/H_2O (4:1 v/v) at pH = 7.4, (MOPS buffer, $1.0 \cdot 10^{-2}$ M). Since the response of **L1** to Zn^{2+} and Cd^{2+} ions was immediate, time elapsed between additions was only 5 minutes.
Isosbestic points at 390, 357, 325, 298 nm and 387, 355, 335, 325, 297, 263, 251 and 228 nm were observed for Zn^{2+} and Cd^{2+}, respectively (Fig. 4a and S3a, ESI), whereas spectrofluorimetric titrations confirmed a 47-fold and 45-fold fluorescence emission enhancement following the addition of 1 equiv. of Zn^{2+} (Φ = 0.13) and 1 equiv. of Cd^{2+} (Φ = 0.11), respectively (Fig. 4b and S3b, ESI). Both the absorbance and fluorescence intensity/molar ratio plots suggest a 1:1 metal-to-ligand stoichiometry in solution (insets of Fig. 4 and S3, ESI).
The same emission maximum observed for free **L1** and its metal complexes (Fig. S2, ESI) suggests a fluorescence transition from an identical excited state in the presence or absence of the metal cations (no ratiometric response), that, together with the metal-induced fluorescence enhancement, reveals an unusual behavior for an ESIPT chromophore, as already pointed out by Kwon and co-workers [53].

<Insert Figure 4>

The same new absorption and emission bands that appeared and increased with the addition of Zn^{2+} and Cd^{2+} ions, were also observed when an excess of tetramethylammonium hydroxide was added to a solution of **L1** (MeCN/H_2O, 4:1 v/v) (Fig. S4, ESI), so that it can be suggested that the coordination of the two metal ions causes the deprotonation of **L1** under the experimental conditions and the deprotonated form is responsible for the UV-Vis and fluorescence emission spectral changes.

In a typical ESIPT sensor, metal coordination suppresses the ESIPT mechanism, resulting in enol-fluorescence, that is hypsochromically shifted with respect to the keto-fluorescence: ratiometric signals can be therefore achieved. In

the present case, since no ratiometric response was observed, we can hypothesize that intramolecular photoinduced electron transfer (PET) occurs from the aliphatic amine to HNBO in the metal-free form of the ligand, which ends to be substantially non-emissive. A cation such as Zn^{2+} or Cd^{2+} facilitates the deprotonation of the naphthol group, and the consequent metal coordination prevents the intramolecular PET because of the nitrogen lone pair energy lowering coupled with the increasing of the HOMO energy level of the deprotonated fluorophore, leading to a fluorescence turn-on, independently of the keto-enol tautomerism.

The emission of free **L1** is low at all pH values in the medium considered; this aspect suggests that another quenching mechanism besides PET might be at work. Previous studies on HNBO-based ligands [53] suggest that a twisted intramolecular charge transfer (TICT) may be the reason for the scarcely emissive species at high pH, whereas a partial PET process may occur from the macrocyclic unit at low pH. This hypothesis is in line with our findings, since both mechanisms would be prohibited by metal coordination, switching on the fluorescence emission. All the studied metal ions except Al^{3+} are able to modify the UV-Vis spectrum of **L1** (Fig. S1, ESI), meaning that they are coordinated by the ligand; however, not all of them increase the fluorescence emission, in particular Cu^{2+} and Co^{2+}, besides Al^{3+} (Fig. 3). Nevertheless, only Zn^{2+} and Cd^{2+} provide an immediate fluorescence response by **L1**.

The ion competition was studied in MeCN/H_2O (4:1 v/v) at pH = 7.4 (MOPS buffer, $1.0 \cdot 10^{-2}$ M). Different types of measurements were performed for this purpose on **L1**, all of them leading to the same results (Fig. 5). Analysis were performed either by adding 1 equiv. of Zn^{2+} to a solution containing **L1** and M^{n+} (M^{n+} = Cd^{2+}, Co^{2+}, Cu^{2+}, Fe^{3+}, Hg^{2+}, K^{+}, Mg^{2+}, Al^{3+}, Ni^{2+} and Pb^{2+}) in equimolar amounts (Scheme S1a, ESI) or by adding 5 equivs. of M^{n+} to an equimolar solution of **L1** and Zn^{2+} (Scheme S1b, ESI). In both cases, only the addition of Cu^{2+} and Hg^{2+} solutions causes a considerable drop of the fluorescence emission, suggesting a competition with the Zn^{2+} ion for the binding to **L1**. Noteworthy, five days are needed to obtain this result when adding M^{n+} to an equimolar **L1**/Zn^{2+} mixture (five days), while the response is immediate when adding Zn^{2+} to a **L1**/M^{n+} mixture, despite the 1:5 **L1**/M^{n+} molar ratio. This suggests that when the **L1**-Zn^{2+}

complex is not pre-formed in solution, **L1** immediately forms the thermodynamically favored complexes with Cu^{2+} and Hg^{2+} (experiment a in Scheme S1, ESI), whereas a kinetic control takes place when a metal cation is added to the preformed **L1**-Zn^{2+} complex, leading to the more thermodynamically stable complex with elapse of time (experiment b in Scheme S1, ESI).

<Insert Figure 5>

Ion competition studies were also performed by adding **L1** to a mixture of 1 equiv. of all metal ions (Zn^{2+}, Cd^{2+}, Co^{2+}, Cu^{2+}, Fe^{3+}, Hg^{2+}, K^{+}, Mg^{2+}, Al^{3+}, Ni^{2+} and Pb^{2+}). Since Hg^{2+} affects the most the emission of the system, a parallel experiment was conducted in the same conditions without Hg^{2+} ion. The complete mixture of metal ions, both in the absence and presence of Zn^{2+} or Cd^{2+}, greatly reduces the fluorescence emission increase previously observed for **L1** upon the addition of only Zn^{2+} or Cd^{2+} (Fig. S5a, ESI), just like the sole Hg^{2+} species does. When Hg^{2+} is not present in solution the fluorescence emission in the presence of all other metal ions, included Zn^{2+} and/or Cd^{2+}, is only marginally affected with respect to the equimolar **L1**/Zn^{2+} or **L1**/Cd^{2+} mixtures emission (Fig. S5b, ESI), meaning that there is not substantial interference by metal cations other than Hg^{2+} when they are in a mixture.

From these data, it can be deduced that Hg^{2+} forms a more stable complex with **L1** with respect to Zn^{2+} and Cd^{2+}, even in competition with all other tested metal cations. This behavior agrees with Hg^{2+} being softer compared to Zn^{2+} and Cd^{2+} thus having higher affinity toward sulfur donor ligands. Interestingly enough, the co-presence of Zn^{2+} and Cd^{2+} ions in solution switches on the system even in the presence of Hg^{2+} (Fig. S5a, ESI), contrarily to what the sole Zn^{2+} and Cd^{2+} ions do. This notwithstanding, the reached intensity is lower than that observed for the equimolar **L1**/Zn^{2+} or **L1**/Cd^{2+} mixtures.

Metal complexation by L2

The UV-Vis absorption spectrum of a solution of **L2** in MeCN/H_2O (4:1 v/v) solution presents a broad band at 360 nm (ε = 18640 $mol^{-1}dm^3cm^{-1}$) and two shoulders at 276 (ε = 6050 $mol^{-1}dm^3cm^{-1}$) and 232 nm (ε = 15580 $mol^{-1}dm^3cm^{-1}$), respectively. Significant changes in the UV-Vis spectrum of **L2** in MeCN/H_2O (4:1 v/v) at pH = 7.4 (MOPS buffer, $1.0 \cdot 10^{-2}$ M) were observed only

upon addition of Cd^{2+}, Cu^{2+} and Hg^{2+} ions. Particularly, the band at 360 nm decreased, whereas a new band appeared at about 330 nm (Fig. S6, ESI). In MeCN/H_2O (4:1 v/v) solution, **L2** exhibits an emission band at 433 nm when excited at 340 nm with a fluorescence quantum yield Φ = 0.091. Interestingly, only upon addition of Cd^{2+} at pH = 7.4 (MOPS buffer, $1.0 \cdot 10^{-2}$ M), a significant CHEF effect was observed (Fig. 6).

<Insert Figure 6>

The optical selectivity for Cd^{2+} displayed by **L2** prompted us to further investigate the binding properties of this ligand towards metal ions. A spectrophotometric titration of **L2** with Cd^{2+} in MeCN/H_2O (4:1 v/v) at pH = 7.4, showed the formation of three isosbestic points at 240, 265 and 340 nm (Fig. 7a), while a spectrofluorimetric titration under the same experimental conditions confirmed the significant selective CHEF effect at 433 nm (Fig. 7b). The fluorescence emission intensity reached the maximum after the addition of about 0.8 equiv. of Cd^{2+} ion, with a quantum yield Φ = 0.22. The inflection points in both the absorbance and fluorescence intensity/molar ratio plots (insets of Fig. 7a and 7b) would suggest the formation in solution of a 1:1 metal-to-ligand complex.

<Insert Figure 7>

Ion competition was studied in MeCN/H_2O (4:1 v/v) at pH = 7.4 (Fig. 8). As in the case of **L1**, two types of measurements were performed, either by adding 5 equivs. of M^{n+} to an equimolar solution of **L2** and Cd^{2+} or by adding 1 equiv. of Cd^{2+} to an equimolar solution of **L2** and M^{n+}. In both cases the same results were obtained, attesting that Cu^{2+} and Hg^{2+} are capable to compete with Cd^{2+} in binding to **L2**.

<Insert Figure 8>

NMR-measurements

In order to gain a deeper insight into the nature of the Zn^{2+} and Cd^{2+} complexes with **L1** and the Cd^{2+} complex with **L2** responsible for the CHEF effect observed, we analyzed the complexation of these metal cations by means of ^1H NMR measurements. While the MeCN/H_2O (4:1 v/v) solvent mixture resulted optimal at the low concentration used in UV-Vis and fluorescence emission

measurements, it could not be used at the higher metal and ligand concentrations required for ^{1}H NMR measurements (concentration *ca* 0.01 M). Both ligands showed low solubility in $MeCN/H_2O$ mixtures and, therefore, the spectra were recorded in solvent media adequate to overcome this problem: DMSO-d_6, for **L1**, and $CD_3CN/CDCl_3$ (7:3 v/v), for **L2**.

L1. The ^{1}H NMR and ^{13}C NMR spectra of **L1** in DMSO-d_6, exhibit, respectively, eleven aromatic and four aliphatic ^{1}H proton resonances, in addition to the -OH signal (see the Experimental Section, Fig. 9a and ESI), and a total of twenty-four ^{13}C signals, twenty for the aromatic and four for the aliphatic carbon resonances, suggesting a C_s symmetry for **L1** mediated on the NMR time scale. The ^{1}H NMR spectrum obtained upon the addition to **L1** in DMSO-d_6 of 1 equiv. of Zn^{2+} as perchlorate salt shows an increase in proton signals, ascribable to the presence of two species in solution (Fig. 9b). The stack-plot of the spectra obtained by step-by-step addition of Zn^{2+} is reported in Fig. S7, ESI. One pattern of signals is attributed to free **L1** (black circles in Fig. 9b), whereas the other to the $[Zn(H_{-1}\mathbf{L1})]^{+}$ complex species (*vide infra*) (black stars in Fig. 9b).

<Insert Figure 9>

Looking at the aliphatic resonances belonging to free **L1** (*H*4-*H*7), they undergo a downfield shift and a broadening as compared to those of free **L1** in the absence of Zn^{2+} (Table S1, ESI). This behavior can be interpreted by considering the protonation of free **L1** as a consequence of the metal ion coordination, to give the $(H\mathbf{L1})^{+}$ species. Such a process would be induced by the presence of Zn^{2+}. Indeed, as already described, the coordination of Zn^{2+} ion to **L1** causes the deprotonation of the naphthol group of **L1** in a buffered $MeCN/H_2O$ medium. Thus, in the absence of a buffer, the naphthol acidic proton produced by the coordination of Zn^{2+} would be neutralized by the tertiary amine function of the **L** moiety of a second molecule of free ligand to form the $(H\mathbf{L1})^{+}$ species. As a consequence, a mixture of $[Zn(H_{-1}\mathbf{L1})]^{+}$ and $(H\mathbf{L1})^{+}$ species is present in solution (Scheme 2). This hypothesis is confirmed by the ^{1}H NMR spectrum of **L1** in DMSO-d_6 at acidic pH values (DCl) (Fig. S8, ESI), whose resonances correspond to those attributed to the $(H\mathbf{L1})^{+}$ species in Fig. 9b.

<Insert Scheme 2>

In order to further support this hypothesis and to help the complete deprotonation process of **L1** upon Zn^{2+} binding, 1 equiv. of Bu_4NOH was added to the **L1**/Zn^{2+} system in DMSO-d_6; upon the addition, the resonances attributed to the (H**L1**)$^+$ species disappeared while only those attributed to the [Zn(H_{-1}**L1**)]$^+$ species remained in the spectrum (Fig. 9b, black stars, and Fig. 9c). The same spectrum was obtained by adding Zn^{2+} to the deprotonated species of the ligand (H_{-1}**L1**)$^-$ (obtained upon the addition of 1 equiv. of Bu_4NOH to **L1** in DMSO-d_6) (Fig. S9b, ESI). The comparison between spectra of [Zn(H_{-1}**L1**)]$^+$ and (H_{-1}**L1**)$^-$ (Fig. S9, ESI) highlights that the aromatic protons *H1, H2* (pyridine), *H11* and *H16* (HNBO moiety) and all the aliphatic protons exhibit the main shift upon zinc complexation (Table S1, ESI). More in detail, the singlet attributed to the *H*4 resonance in deprotonated **L1** undergoes a downfield shift and splits in a characteristic AB system due to two non-equivalent protons of a -CH_2 group; this clearly evidences the stiffening of the macrocycle moiety upon Zn^{2+} ion complexation. The same loss of equivalence due to the stiffening of the macrocyclic ring, on the NMR time scale, can be observed for the *H*5 and *H*6 aliphatic resonances, which split in four multiplets, due to the coupling between non-degenerate methylene protons. The shift of the aromatic signals suggests that also the deprotonated HNBO as well as the pyridine fragments are involved in the stabilization of the Zn^{2+} ion through the naphtholate oxygen and pyridine nitrogen atoms. Consequently, looking at all proton and carbon signals, it can be hypothesized that in these conditions the whole **L** macrocyclic unit, *via* the N_2S_2 donor set, along with the deprotonated HNBO moiety are involved in the coordination of the Zn^{2+} ion to form the [Zn(H_{-1}**L1**)]$^+$ complex.

The ^{1}H NMR spectrum acquired upon the addition of 1 equiv. of Cd^{2+} as perchlorate salt mainly shows the free ligand signals, along with very weak resonances ascribable to the [Cd(H_{-1}**L1**)]$^+$ complex and to the protonated (H**L1**)$^+$ species (Fig. S10, ESI). The highly coordinating DMSO solvent strongly compete with **L1** for the coordination of the large Cd^{2+} ion, preventing considerable formation of [Cd(H_{-1}**L1**)]$^+$ complex. As in the case of Zn^{2+}, the addition of 1 equiv. of Bu_4NOH favors the deprotonation of the naphthol and the complexation of the Cd^{2+} cation. Indeed, upon the addition of the base the signals of [Cd(H_{-1}**L1**)]$^+$ complex increase and prevail on those of the free ligand, that are however still

visible, suggesting a lower affinity of Cd^{2+} than Zn^{2+} for the $(H_{-1}\mathbf{L1})^-$ species, at least in DMSO. The ^1H NMR spectrum of $[Cd(H_{-1}\mathbf{L1})]^+$ complex shows a pattern similar to that of the $[Zn(H_{-1}\mathbf{L1})]^+$ complex, suggesting for the two complexes a similar coordination environment. In the case of the Cd^{2+} complex, signals are however broader, denoting high fluxionality of the species on the NMR time scale probably due to the larger size of the Cd^{2+} ion compared to Zn^{2+}.

L2. In the case of **L2**, the analysis of the NMR spectra shows that the addition of one equivalent of Cd^{2+} to **L2** causes a reduction of the symmetry of the macrocyclic **L** moiety, similarly to what observed in the case of **L1**. The singlet attributed to the *H*4 resonance undergoes a downfield shift and splits in the characteristic AB system (Fig. 10). The same loss of equivalence due to the stiffening of the macrocyclic ring, can be observed for the *H*5 and *H*6 aliphatic resonances. In fact, both the aliphatic ^1H resonances of **L2** at 2.51 and 3.80 ppm, assigned to protons *H5–H6* and *H4*, respectively, split into two distinct series of signals clearly attributable to the coordination of the Cd^{2+} by the **L** moiety (N_2S_2 core, Fig. 10).

<Insert Figure 10>

Interestingly, the singlet at 2.51 ppm (*H5–H6*) splits into four multiplets at 3.16, 2.79, 2.56 and 2.31 ppm, each integrating for two protons and the singlet at 3.80 (*H4*) splits into two doublets at 4.35 and 4.11 ppm, integrating each for two protons. The dramatic high-frequency shift ($\Delta\delta$ = 0.87 ppm) experienced by the signal assigned to the secondary NH, suggests the coordination of this amine group to the metal ion. With regard to the two signals of the $–CH_2–CH_2–$ spacer (*H7* and *H8*), the one closer to the nitrogen of the macrocyclic **L** moiety (*H7*) shows a greater shift compared to the *H8* proton ($\Delta\delta$ = 0.35 and 0.23 ppm, respectively) (Fig. 10 and Table S2, ESI).

Noteworthy, shifts to higher frequency of the aromatic coumarin protons were also observed (Table S2, ESI). These are probably due to the electronic rearrangement over the coumarin moiety, as a consequence of the metal coordination. As a matter of fact, these results show that Cd^{2+} coordination occurs in solution through the N_2S_2 core of the macrocyclic **L** moiety, most likely with the

participation of the NH secondary amine group, while coumarin oxygen atoms do not seem to be involved in the interaction.

Solid state characterization

After several attempts to obtain crystals suitable for X-ray diffraction analysis of the Zn^{2+} and Cd^{2+} metal complexes of **L1** and **L2**, we were able to grow pale yellow single crystals only for the complex [Cd**L2**$(NO_3)_2$] (**1**) by Et_2O diffusion in a DMF solution of the compound (see ESI for selected bond distances and angles and crystallographic details, Tables S3 and S4, ESI). Fig. 11 shows the coordination sphere around the metal center, where four positions are occupied by the N_2S_2-donor set of the macrocyclic framework [Cd1–N1 2.419(2), Cd1–N2 2.532(2), Cd1–S1 2.6555(4), Cd1–S2 2.6450(4) Å)] and two sites are taken up respectively by a monodentate [Cd1–O11 2.359(2) Å] and a slightly asymmetric bidentate NO_3^- [Cd1–O14 2.584(2), Cd1–O8 2.420(2) Å] anionic ligands, to give an overall $N_2S_2O_3$-heptacoordination at the metal center. A similar heptacoordination at the Cd^{2+} center has been observed in complexes with aliphatic tetradentate mixed donor macrocycles [55].

<Insert Figure 11>

As already observed for [Cu**L**$(NO_3)_2$] and [Zn**L**$(NO_3)_2$] in [38], the macrocyclic framework of **L2** adopts a folded conformation resembling an open book with the spine along the line connecting the S1–Cd1–S2 atoms and the N1–Cd1–N2 hinge angle of 81.20(5)°. The aliphatic tertiary nitrogen is therefore located almost perpendicularly to the pseudo-plane defined by the metal ion, the pyridine ring and the S-donors. In the solid state the secondary N-donor belonging to the pendant arm is not involved in the metal coordination, as contrary to what observed in the structurally characterized complexes of $\mathbf{L_C}$-$\mathbf{L_E}$ in which the donor groups from the pendant arm are directly involved in metal coordination both in solution and in the solid state [39]. In the case of **L2** in solution, at least in the solvent mixture used for NMR measurements, it is likely that the secondary N-donor from the pendant arm takes the place of one coordinated anion in the coordination sphere of the metal.

Development of solvent polymeric membrane optodes based on ligands L1 and L2 for selective Cd^{2+} detection

Very recently, based on preliminary studies on the sensing properties of **L1** and **L2**, we have employed these two fluorescent chemosensors to develop an optical sensor array implemented with familiar devices for signal acquisition (Light Emitting Diode, LED, as light source and a digital web-camera as a signal detector) in combination with chemometric methods for data treatment for the measurement of Cd^{2+} and NO_2^- in natural water samples [47]. Encouraged by the accurate selectivity data and deep knowledge of the coordination behavior of **L1** and **L2** obtained in solution in the present study, we have investigated the possibility to go a step forward developing solvent polymeric membrane optodes based on the chemosensors **L1** and **L2**, and combining them with the familiar Photoassisted Technique (PT) to afford new optical sensor devices for selective detection of Cd^{2+} in different real samples. In particular we have considered soil samples for the new analytical application of **L1** and **L2**.

Since both **L1** and **L2** exhibit a notable absorbance in the range from 360 to 450 nm, we have employed a commercially available blue-colored Light Emitting Diode (LED, λ_{ex} = 380nm) as a single monochromic light source for optical sensors excitation To test **L1** and **L2** for the development of this kind of sensor devices, a series of PVC-based polymeric membranes were prepared employing three different plasticizers, DOS (bis(2-ethylhexyl) sebacate), oNPOE (o-nitrophenyl octyl ether) and TOP (tris(2-ethylhexyl)phosphate), and potassium tetrakis-(4-chlorophenyl)borate (TpClPBK) as a lipophilic anionic additive. Since **L1** and **L2** are expected to act inside polymeric membranes as neutral-carriers binding the charged Cd^{2+} ions, the inclusion of TpClPBK cation-exchanger inside tested membranes was required in order to induce the flux of the ions into the membrane and to tune the ion-exchange properties [43,47]. In total 12 membranes of different compositions, namely membranes Mb1-Mb6 based on **L1**, and membranes Mb7-Mb12 based on **L2**, were prepared and tested (Table 1). The membranes were cast onto a transparent glass slide support by drop casting method; in order to guarantee the reproducibility of the measurements, 2 to 4 sensing spots for every membrane were deposited on the same glass support.

<Insert Table 1>

Initially, the membrane responses were studied in several 0.01 M buffer background water solutions with different pH (in MES at pH 5.5, HEPES at pH 7.5 and TRIS at pH 8.6), in order to determine the background composition and pH influence on the optodes response. It was observed that at pH 5.5 in MES buffer background almost all the tested membranes were non-responsive, even in the presence of high concentrations ($>1.0 \cdot 10^{-3}$ M) of Cd^{2+} analyte. The highest variation of optical intensity of **L1**-based membranes Mb1-Mb6 (Table 1) was found in TRIS buffered solution at pH 8.6, where the basic medium promotes the deprotonation of the fluorophore. In fact, as already discussed, basic conditions promote ligand deprotonation and favor the complexation of the target cation *via* the formation of a 1:1 metal-to-ligand complex. Unfortunately, the precipitation of metal hydroxide species did not permit to test membrane responses in a wide concentration range at pH 8.6 (TRIS buffer). Therefore, for further investigations, pH 7.5 conditions (0.01 M HEPES) were chosen, corresponding to those typical for environmental samples, such as surface waters and soils (pH range 5.6–8.4). In order to promote an initial **L1** fluorophore deprotonation, the functionalized glass slides were soaked into a solution at pH 8.6 (0.01 M TRIS) for 15 min, then rinsed with distilled water and immersed into a solution at pH 7.5 (0.01 M HEPES), where consecutive additions of analyte were made. Membrane selectivity tests towards several cations, namely Li^+, Na^+, K^+, Mg^{2+}, Ca^{2+}, Co^{2+}, Cu^{2+}, Zn^{2+}, Cd^{2+}, Pb^{2+} and NH_4^+, were performed under these conditions.

No useful response was found for membranes Mb1 and Mb7 based on **L1** and **L2**, respectively, without lipophilic anionic sites, while the oNPOE-plasticized membranes Mb2, Mb3, Mb8 and Mb9 showed a very low optical response, due to the fluorophores luminescence quenching by the plasticizer, in agreement with previous evidences [43]. Considering that the formation of a 1:1 metal-to-ligand complex is prevalent in MeCN/H_2O 4:1 (v/v) solutions for both **L1** and **L2**, an excess of lipophilic anions molar content (at least twice the molar concentration) with respect to the carrier concentration is required to guarantee the cations flux inside the membrane and an efficient ion-exchange. In fact, the addition of 2-5 wt.% of TpClPBK in membranes Mb4, Mb5 and of 2-8 wt.% of TpClPBK in Mb10, Mb11 doped with **L1** and **L2**, respectively, resulted in a significant membranes

luminescence variation in solutions of Cd^{2+} ion in the concentration range from $3.3 \cdot 10^{-7}$ to $5.0 \cdot 10^{-3}$ M and in binary solutions containing a fixed amount of Cd^{2+} ($5.0 \cdot 10^{-3}$ M) and a variable concentration of Zn^{2+} ions ($5.0 \cdot 10^{-5}$ – $3.2 \cdot 10^{-3}$ M) at pH 7.5 buffer background (0.01 M HEPES) (Fig. 12). Such a behavior indicates a neutral carrier functioning mechanism of ligands inside a polymeric membrane phase [43].

<Insert Figure 12>

The **L1**-doped membranes Mb4 and Mb5 demonstrated a luminescence increase in the presence of Cd^{2+} for concentrations higher than 0.1 mM; these membranes also responded to Zn^{2+} for lower or almost equal concentrations of the metal ion (Fig. 12).

A relatively low fluorescence response variation was observed for **L2**-based membranes Mb10 and Mb11 (Fig. 12) at different concentrations of Cd^{2+}. Thus, Mb10 containing 1 wt.% of **L2** showed a slight luminescence increase upon increasing the Cd^{2+} concentration, while higher percentage of ligand (3 wt.%) in Mb11 provoked a complete saturation of the membrane luminescence at $[Cd^{2+}] > 5.0 \cdot 10^{-5}$ M. For this reason, further tests were performed with membranes doped with 1 wt.% of **L2**.

Another important membrane component strongly influencing the sensitivity of the membrane optodes is the plasticizer, because it improves the permeability, reduces the frailness, and tunes the fluorescence emission intensity [43,56]. The plasticizer polarity is mainly responsible for dissociation of membrane-active components and uniform ligand distribution inside the membrane phase, and for the target ion exchange processes among the membrane and the analyzed sample solution. Due to the fact that oNPOE, the plasticizer with the highest polarity ($\varepsilon_{oNPOE} = 23.9$ *vs* $\varepsilon_{DOS} = 3.9$), is optically active and it was involved in fluorophores luminescence quenching in membranes Mb2, Mb3, Mb8 and Mb9 (see above), the properties of membranes plasticized with TOP ($\varepsilon_{TOP} = 4.8$) were considered (Mb6 and Mb12 in Table 1) [57].

In Fig. 13 the normalized PT response, obtained as the difference of optical intensities at the green channel, for all the tested cations in two solutions with concentrations $1.0 \cdot 10^{-3}$ M and $1.0 \cdot 10^{-7}$ M at pH 7.5 (0.01 M HEPES buffer) is

shown for the studied DOS- and TOP-plasticized membranes. TOP-plasticized membranes Mb6 and Mb12 exhibited the highest fluorescence intensity variation in the presence of several tested cations, and among them Cd^{2+} showed the highest response under the experimental conditions used.

<Insert Figure 13>

No significant fluorescence changes were observed for DOS-plasticized membranes upon addition of increasing concentrations of alkali metal (Na^+, Li^+, K^+), ammonium (NH_4^+) and Ca^{2+} ions. The only notable luminescence enhancement of **L2**-based membranes Mb10 and Mb11 was registered in the presence of Mg^{2+}. This response to Mg^{2+} was almost deteriorated in the TOP-plasticized membrane Mb12, for which a partial response to Li^+ was registered instead. The **L1**-based membrane Mb6 prepared with TOP showed the highest luminescence variation upon Cd^{2+} binding, with a significant response to Zn^{2+} and a lesser influence of Pb^{2+}, Na^+ and K^+ ions.

It is interesting to note the inverse response of TOP-plasticized **L2**-based membrane Mb12, for which the negative gradient of optical intensity indicates a quenching of the film emission upon Cd^{2+} exposure as compared to the enhancement of the fluorescence emission in the case of the **L1**-based membrane Mb6. These results are in agreement with our recent study dedicated to the application of a fluorescent sensor array based on several fluorophores, comprising **L1** and **L2**, for pollutants detection in natural waters [47].

In the present work we have checked the practical applicability of the developed membrane optodes based on **L1** and **L2** chemosensors for the selective Cd^{2+} detection in aqueous extracts from soil samples. The natural cadmium content in soils of upper 20 cm depth is normally in the range 0.2-0.4 mg/kg, which corresponds to approximately a $1.0 \cdot 10^{-5}$ M concentration [58]. In order to evaluate the performance of the proposed sensors in complex multicomponent media, containing several interfering species, the amount of Cd^{2+} in three soil samples from three Italian sites with different anthropogenic influences (Sample 1 was from a site close to the landing strip of Ciampino G.B. Pastine airport, Rome; Sample 2 was from the garden of the Faculty of Science, "Tor Vergata" University in Rome (Sogene building); Sample 3 was from waste

dump from Castello di Cisterna, Naples) has been detected. Recovery experiments were carried out by standard addition method consisting in two consecutive additions of a known concentration of Cd^{2+} ion (as chloride salt) in the analyzed soil aqueous extract. The luminescence variation of optical sensor films was detected with PT technique. The optodes were prepared with **L1**- and **L2**-based membranes Mb6 and Mb12, respectively, which showed the highest sensitivity to Cd^{2+} ions. In total four sensing spots (two per membrane) were deposited on the same glass slide; the membranes were stored in the dark prior to use, the new disposable optical sensor was employed for every measurement. The optical intensities of every sensing spot in respect to the red (at about 630 nm) and green color (at about 530 nm) constituents of visible spectrum (see experimental section for more details) were measured in the presence of increasing Cd^{2+} concentrations in order to obtain optodes calibration curves.

Fig. 14 clearly shows an evident difference among the tested samples in terms of Cd^{2+} presence. Moreover, through referring to the Cd^{2+} calibration photogram, an initial semi-qualitative insight on the Cd^{2+} amount in analyzed soil samples could be done. Thus, a visually evident similarity between Sample 1 and 0.001 M Cd^{2+} calibration solution (reported at the top image of Fig. 14) and a lower concentration of Cd^{2+} in soil Samples 2 and 3 (at about $1.0 \cdot 10^{-5}$ M level) for Mb6 based on **L1** can be noticed. For **L2**-based Mb12, the differences in luminescence intensity are less evident for visual comparison; only an enhanced luminescence in Sample 2 is visible to the naked-eye, indicating a lower Cd^{2+} content in comparison to the other two tested samples. This founding is reasonable, considering the Sample 2 provenance (presumably an unpolluted zone: university garden) in comparison to the other two samples (airport landing line and waste dump for Samples 1 and 3, respectively).

<Insert Figure 14>

For Cd^{2+} quantification, we have tested responses of both separate optodes based on Mb6 and Mb12 with the best performances and of their multisensory arrangement (see ESI for details of multisensor array preparation), where the responses of all optodes are treated together to obtain a multivariate regression model. The standard calibration curve method was applied for the

single optodes, whereas the regression method was used to obtain the correlation between the PT responses and the Cd^{2+} ion content in calibration solutions of known concentrations. The final data set was composed of 2 membranes × 3 replicates × 2 light channels (RG) × 6 Cd^{2+} ion concentrations: 72 points in total used for the PLS1 regression model construction. Since the membrane luminescence intensity variation in the blue channel was negligible, it was not considered for data treatment. As far as the single optodes were concerned, the best performance was found for Mb6, based on **L1** registering the optical intensity variation in the green channel. The analytical results obtained for this membrane (and for the multisensory array) are outlined in Table 2.

<Insert Table 2>

The amounts of Cd^{2+} in aqueous extracts of soil samples found with single **L1**-based optode were in agreement with the Cd^{2+} content estimated with standard AAS method. The lower Cd^{2+} amount in soils aqueous extracts obtained with optodes is due to the quantification of free Cd^{2+} activity in comparison to AAS results providing the total Cd^{2+} content. Analogously, the sensor array provided even lower values for Cd^{2+} concentration for all tested soils, with respect to the AAS technique and selective optode with **L1**-based membrane Mb6. We can explain such a result by the high influence (expressed by highest loadings) of **L2**-based membrane Mb12 on the sensor array output. The response of membrane Mb12, cross-sensitive to Zn^{2+}, Cu^{2+} and Pb^{2+} cations (Fig. 13), in soil extracts, which are the complex solutions of several ionic species passed from solid soil phase to liquid extract, is influenced by this multicomponent composition. This is especially evident for the most polluted soil Samples 1 and 3 collected in airport and waste dump respectively (Table 2).

An application of optical sensor array in soil Samples 2 and 3 has provided even a better precision with the recoveries laying in a narrow range from 98.5% to 100.5%, and mean RSD of 0.96 %, while the detection of the Cd^{2+} amount spiked in Sample 1 was not possible due to the high initial concentration of analyte [59]. The correlation coefficients, R^2, of PLS1 model constructed, which relate the output of the sensor array response to the amounts of Cd^{2+} ion in calibration solutions, were 0.993 and 0.983 for calibration and validation steps,

respectively, and the Root Mean Squared Error of Validation, RMSEV, was 0.225 in -log[Cd^{2+}] units (Fig. 15a). Model was fitted with 3PCs, representing 99.3% and 98.1% of total explained variance at calibration and validation steps respectively (Fig. 15b). A detection limit of $1.8 \cdot 10^{-7}$ M for Cd^{2+} ion was estimated by the 3σ method (DL = $3\sigma/S$ where σ is the RMSEV calculated in M and S = 0.993 is the slope of the regression line at calibration stage).

<Insert Figure 15>

The obtained DL value is three orders of magnitude lower than the USEPA (U.S. Environmental Protection Agency) value of 20 mg/kg (corresponding to $1.8 \cdot 10^{-4}$ M) for Cd^{2+} in the agricultural topsoils, that represents no significant health risk to individuals through dietary ingestion of Cd^{2+}-contaminated food crops [60], also considering WHO/FAO (World Health Organization/Food and Agriculture Organization of United Nations) recommended maximum tolerable value for Cd^{2+} entering in diets from soils and crops (25 μg/kg body weight per month) [61].

Conclusions

In this paper, the macrocycle 2,8-dithia-5-aza-2,6-pyridinophane (**L**) was considered as a receptor unit in the development of conjugated fluorescent chemosensors, further demonstrating the efficacy of the "complementary synthetic strategy" in reaching at least an optical selectivity towards heavy metal ions. In particular, the optical selectivity and coordination properties towards Cd^{2+} and Zn^{2+} of two **L**-based chemosensors **L1** and **L2** differing in the signaling units have been deeply investigated. The addition of Zn^{2+} and Cd^{2+} ions induces the deprotonation of the naphthol chromophore of **L1** and a fluorescence turn-on, which can be explained by suppression of PET rather than by ESIPT mechanism. Similarly, a significant CHEF effect was observed for **L2**, but only upon addition of Cd^{2+}. In both cases, the formation of 1:1 metal-to-ligand complexes is observed.
Despite these chemosensors lack of a thermodynamic selectivity in the binding process, their optical selectivity has allowed for the preparation of sensitive materials when supported in PVC-based polymeric membranes. Several membranes, differing for the plasticizer type and the cation-exchanger amount, were cast onto transparent glass slide supports and tested at different pH values.

The TOP-plasticized Mb6 and Mb12 doped with **L1** and **L2**, respectively, resulted the most promising among all tested membranes, showing the highest fluorescence intensity variation for Cd^{2+} at pH 7.5. Notably, **L2**-based membrane Mb12 shows a quenching of the film emission upon Cd^{2+} exposure that is an inverse response compared to the enhancement of the fluorescence emission in the case of the **L1**-based membrane Mb6.

The new sensor devices have been successfully used in a fluorescent sensor array for the quantitative determination of Cd^{2+} ions in real samples of environmental importance such as soils of different provenance, once combined with the Photoassisted Technique (PT) for signal acquisition. The amounts of Cd^{2+} in aqueous extracts of soil samples found with single **L1**-based optode were in agreement with the Cd^{2+} content estimated with standard AAS method ($[Cd^{2+}]_{Mb6}$ = 0.511, 0.007, 0.024 mg/kg *vs* $[Cd^{2+}]_{AAS}$ = 0.574, 0.010, 0.030 mg/kg for airport, garden and waste dump samples, respectively) and with that found with the sensor array ($[Cd^{2+}]_{sa}$ = 0.452, 0.005, 0.019 mg/kg). The obtained detection limit of $1.8 \cdot 10^{-7}$ M for Cd^{2+} ion is three times lower than that recommended from the USEPA, corresponding to $1.8 \cdot 10^{-4}$ M of Cd^{2+} in the agricultural topsoils. We would like to underline that for analytical application, fluorescent chemosensors do not necessarily have to possess both thermodynamic and optical selectivity for the target analytes, this simplifies the approach to the design and the synthetic process to adopt in the development of sensitive optical materials.

Conflicts of interest

There are no conflicts to declare.

Acknowledgements

This research was funded by the Italian Ministero dell'Istruzione dell'Università e della Ricerca (MIUR) (project 2017EKCS35). We thank also Fondazione di Sardegna (FdS) (Progetti biennali di Ateneo, Annualità 2018) and the University of Urbino (Department of Pure and Applied Sciences – Grant DISPEA_FUSI_PROG2019, DISPEA_GIORGI_PROG2018) for financial support. Dr.

Luca Piersanti and Dr. Angela Ricci are acknowledged for their assistance with the synthesis of **L1**. Dr. Mattia Nieddu is acknowledged for the synthesis of **L2**.

REFERENCES

[1] (a) A. P. de Silva, T. S. Moodyband, G. D. Wright, Fluorescent PET (Photoinduced Electron Transfer) sensors as potent analytical tools, Analyst 134 (2009) 2385-2393, https://doi.org/10.1039/B912527M; (b) D. W. Domaille, E. L. Que, C. Chang, Synthetic Fluorescent Sensors for Studying the Cell Biology of Metals, Nat. Chem. Biol. 4 (2008) 168-175, https://doi.org/10.1038/nchembio.69

[2] Y. Fan, Y. F. Long, Y. F. Li, A sensitive resonance light scattering spectrometry of trace Hg^{2+} with sulfur ion modified gold nanoparticles, Anal. Chim. Acta 653 (2009) 207-211, 10.1016/j.aca.2009.09.017

[3] P. Pallavicini, L. Pasotti, S. Patroni, Residual and exploitable fluorescence in micellar self-assembled ON–OFF sensors for copper(ii), Dalton Trans. (2007) 5670-5677, https://doi.org/10.1039/B710765J

[4] (a) K. P. Carter, A. M. Young, A. E. Palmer, Fluorescent Sensors for Measuring Metal Ions in Living Systems, Chem. Rev. 114 (2014) 4564-4601, https://doi.org/10.1021/cr400546e; (b) C. Lodeiro, F. Pina, Luminescent and chromogenic molecular probes based on polyamines and related compounds, Coord. Chem. Rev. 253 (2009) 1353-1383, https://doi.org/10.1016/j.ccr.2008.09.008

[5] (a) T. L. Mako, J. M. Racicot, M. Levine, Supramolecular Luminescent Sensors, Chem. Rev. 119 (2019) 322−477, https://doi.org/10.1021/acs.chemrev.8b00260; (b) Jr., J. A. Cotruvo, A. T. Aron, K. M. Ramos-Torresa, C. Chang, Synthetic fluorescent probes for studying copper in biological systems, Chem. Soc. Rev. 44 (2015) 4400-4414, https://doi.org/10.1039/C4CS00346B; (c) J. Zhang, F. Cheng, J. Li, J.-J. Zhu, Y. Lu, Fluorescent nanoprobes for sensing and imaging of metal ions: recent advances and future perspectives, Nano Today 11 (2016) 309-329, https://doi.org/10.1016/j.nantod.2016.05.010

[6] (a) M. Xiao, Z. Liu, N. Xu, L. Jiang, M. Yang, C. Yi, A Smartphone-Based Sensing System for On-Site Quantitation of Multiple Heavy Metal Ions Using Fluorescent Carbon Nanodots-Based Microarrays, ACS Sensors 5 (2020) 870-878, https://doi.org/10.1021/acssensors.0c00219; (b) Y. Liu, L.-N. Ma, W.-J. Shi, Y.-K. Lu, L. Hou, Y.-Y. Wang, Four alkaline earth metal (Mg, Ca, Sr, Ba)-based MOFs as multiresponsive fluorescent sensors for Fe^{3+}, Pb^{2+} and Cu^{2+} ions in aqueous solution J. Solid State Chem. 277 (2019) 636-647, https://doi.org/10.1016/j.jssc.2019.07. 020; (c) W. Xu, C. Ren, C. L. Teoh, J. Peng, S. H. Gadre, H.-W. Rhee, C.-L. K. Lee, Y.-T. Chang, An Artificial Tongue Fluorescent Sensor Array for Identification and Quantitation of Various Heavy Metal Ions, Anal. Chem. 86 (2014) 8763-8769, https://doi.org/10.1021/ac501953z; (d) L.-Y. Niu, H. Li, L. Feng, Y.-S. Guan, Y.-Z. Chen, C.-F. Duan, L.-Z. Wu, Y.-F. Guan, C.-H. Tung, Q.-Z. Yang, BODIPY-based fluorometric sensor array for the highly sensitive identification of heavy-metal ions, Anal. Chim. Acta 775 (2013) 93-99, https://doi.org/10.1016/j.aca.2013.03.013; (e) S. Maiti, L. J. Prins, A

modular self-assembled sensing system for heavy metal ions with tunable sensitivity and selectivity, Tetrahedron 73 (2017) 4950-4954, https://doi.org/10.1016/j.tet.2017.05.028
[7] E. M. Nolan, S. J. Lippard, Small-Molecule Fluorescent Sensors for Investigating Zinc Metalloneurochemistry, Acc. Chem. Res. 42 (2009) 193-203, https://doi.org/10.1021/ar8001409
[8] Z. Dai, J. W. Canary, Tailoring tripodal ligands for zinc sensing. New J. Chem. 31 **(**2007) 1708-1718, https://doi.org/10.1039/B710803F
[9] (a) E. L. Que, D. W. Domaille, C. J. Chang, Metals in Neurobiology: Probing Their Chemistry and Biology with Molecular Imaging, Chem. Rev. 108 (2008) 1517-1549, https://doi.org/10.1021/cr078203u; (b) Z. Xu, J. Yoon, D. R. Spring, Fluorescent chemosensors for Zn^{2+}, Chem. Soc. Rev. 39 (2010) 1996-2006, https://doi.org/10.1039/B916287A
[10] A. N. Gusev, V. F. Shul'gin, S. B. Meshkova, S. S. Smola, W. Linert, A novel triazole-based fluorescent chemosensor for Zinc ions J. Lumin. 155 (2014) 311-316, https://doi.org/10.1016/j.jlumin.2014.06.054
[11] R. K. Pathak, V. K. Hinge, A. Rai, D. Panda, C. P. Rao, Imino–Phenolic–Pyridyl Conjugates of Calix[4]arene (L_1 and L_2) as Primary Fluorescence *Switch-on* Sensors for Zn^{2+} in Solution and in HeLa Cells and the Recognition of Pyrophosphate and ATP by [ZnL_2], Inorg. Chem. 51 (2012) 4994-5005, https://doi.org/10.1021/ic202426v
[12] M. Hagimori, T. Uto, N. Mizuyama, T. Temma, Y. Yamaguchi, Y. Tominaga, H. Saji, Fluorescence ON/OFF switching Zn^{2+} sensor based on pyridine–pyridone scaffold, Sens. Actuators B 181 (2013) 823-828, https://doi.org/10.1016/j.snb.2013.02.033
[13] Y. Mikata, A. Takekoshi, M. Kaneda, H. Konno, K. Yasuda, M. Aoyama, S. Tamotsu, Replacement of quinolines with isoquinolines affords target metal ion switching from Zn^{2+} to Cd^{2+} in the fluorescent sensor TQLN (*N*,*N*,*N*′,*N*′-tetrakis(2-quinolylmethyl)-2,6-bis(aminomethyl)pyridine), Dalton Trans. 46 (2017) 632-637, https://doi.org/10.1039/C6DT03948K
[14] M. Taki, M. Desaki, A. Ojida, S. Iyoshi, T. Hirayama, I. Hamachi, Y. Yamamoto, Fluorescence Imaging of Intracellular Cadmium Using a Dual-Excitation Ratiometric Chemosensor, J. Am. Chem. Soc. 130 (2008) 12564-12565, https://doi.org/10.1021/ja803429z
[15] T. Cheng, Y. Xu, S. Zhang, W. Zhu, X. Quian, L. Duan, A Highly Sensitive and Selective OFF-ON Fluorescent Sensor for Cadmium in Aqueous Solution and Living Cell, J. Am. Chem. Soc. 130 (2008) 16160-16161, https://doi.org/10.1021/ja806928n
[16] X. Peng, J. Du, J. Fan, J. Wang, Y. Wu, J. Zhao, S. Sun, T. Xu, A Selective Fluorescent Sensor for Imaging Cd^{2+} in Living Cells, J. Am. Chem. Soc. 129 (2007) 1500-1501, https://doi.org/10.1021/ja0643319
[17] H. N. Kim, W. X. Ren, J. S. Kim, J. Yoon, Fluorescent and colorimetric sensors for detection of lead, cadmium, and mercury ions, J. Chem. Soc. Rev. 41 (2012) 3210-3244, https://doi.org/10.1039/C1CS15245A
[18] S. Ellairaja, R. Manikandan, M. T. Vijayan, S. Rajagopal, V. S. Vasantha, A simple highly sensitive and selective TURN-ON fluorescent chemosensor for the detection of

cadmium ions in physiological conditions, RSC Adv. 5 (2015) 63287-63295, https://doi.org/10.1039/C5RA10612E
[19] (a) S. Goswami, K. Aich, S. Das, C. D. Mukhopadhyay, D. Sarkar, T. K. Mondal, A new visible-light-excitable ICT-CHEF-mediated fluorescence 'turn-on' probe for the selective detection of Cd^{2+} in a mixed aqueous system with live-cell imaging, Dalton Trans. 44 (2015) 5763-5770, https://doi.org/10.1039/C4DT02463J; (b) C. Kar, S. Samanta, S. Goswami, A. Ramesh, G. Das, A single probe to sense Al(III) colorimetrically and Cd(II) by turn-on fluorescence in physiological conditions and live cells, corroborated by X-ray crystallographic and theoretical studies, Dalton Trans. 44 (2015) 4123-4132, https://doi.org/10.1039/C4DT01433B; (c) K. Aich, S. Gonswami, S. Das, C. D. Mukhopadhyay, C. K. Quah, H.-K. Fun, Cd^{2+} Triggered the FRET "ON": A New Molecular Switch for the Ratiometric Detection of Cd^{2+} with Live-Cell Imaging and Bound X-ray Structure, Inorg. Chem. 54 (2015) 7309-7315, https://doi.org/10.1021/acs.inorgchem.5b00784
[20] C. Kumari, D. Sain, A. Kumar, S. Debnath, P. Saha, S. Dey, Intracellular detection of hazardous Cd^{2+} through a fluorescence imaging technique by using a nontoxic coumarin based sensor, Dalton Trans. 46 (2017) 2524-2531, https://doi.org/10.1039/C6DT04833A
[21] Y. Zhang, X. Guo, M. Zheng, R. Yang, H. Yang, L. Jia, M. Yang, A 4,5-quinolimide-based fluorescent sensor for the turn-on detection of Cd^{2+} with live-cell imaging, Org. Biomol. Chem. 15 (2017) 2211-2216, https://doi.org/10.1039/C7OB00201G
[22] (a) R. R. Lauwerys, A. M. Bernard, H. A. Reels, J.-P. Buchet, Cadmium: Exposure markers as predictors of nephrotoxic effects, Clin. Chem. 40 (1994) 1391-1394, https://doi.org/10.1093/clinchem/40.7.1391; (b) S. Satarug, J. R. Baker, S. Urbenjapol, M. Haswell-Elkins, P. E. B. Reilly, D. J. Williams, M. R. Moore, A Global Perspective on Cadmium Pollution and Toxicity in Non-Occupationally Exposed Population, Toxicol. Lett. 137 (2003) 65-83, https://doi.org/10.1016/S0378-4274(02)00381-8 ; (c) M. Waisberg, P. Joseph, B. Hale, D. Beyersmann, Molecular and Cellular Mechanisms of Cadmium Carcinogenesis, Toxicology 192 (2003) 95-117, https://doi.org/10.1016/S0300-483X(03)00305-6 ; (d) R. K. Zalups, S. Ahmad, Molecular Handling of Cadmium in Transporting Epithelia, Toxicol. Appl. Pharmacol. 186 (2003) 163-188, https://doi.org/10.1016/S0041-008X(02)00021-2 ; (e) M. Viau, V. Collin-Faure, P. Richaud, J.-L. Ravanat, S. M Candeias, Cadmium and T cell differentiation: limited impact in vivo but significant toxicity in fetal thymus organ culture, Toxicol. Appl. Pharmacol. 223 (2007) 257-266, https://doi.org/10.1016/j.taap.2007.05.017; (f) T. Nawrot, M. Plusquin, J. Hogervorst, H. A. Roels, H. Celis, L. Thijs, J. Vangronsveld, E. Van Hecke, J. A. Staessen, Environmental exposure to cadmium and risk of cancer: a prospective population-based study, Lancet Oncol. 7 (2006) 119-126, https://doi.org/10.1016/S1470-2045(06)70545-9
[23] B. L. Vallee, K. H. Falchuk, The Biochemical Basis of Zinc Physiology, Physiol. Rev. 73 (1993) 79-118, https://doi.org/10.1152/physrev.1993.73.1.79
[24] (a) C. Andreini, I. Bertini, Cavallaro, G. Minimal Functional Sites Allow a Classification of Zinc Sites in Proteins, PLoS ONE 6 (2011) e26325,

https://doi.org/10.1371/journal.pone.0026325 ; (b) C. Andreini, I. Bertini, G. Cavallaro, G. L. Holliday, J. M. Thornton, Metal Ions in Biological Catalysis: From Enzyme Databases to General Principles, J. Biol. Inorg. Chem. 13 (2008) 1205-1218, https://doi.org/10.1007/s00775-008-0404-5
[25] A. I. Bush, The Metallobiology of Alzheimer's Disease, Trends Neurosci. 26 (2003) 207-214, https://doi.org/10.1016/S0166-2236(03)00067-5
[26] C. J. Frederickson, J. Y. Koh, A. I. Bush, The Neurobiology of Zinc in Health and Disease, Nat. Rev. Neurosci. 6 (2005) 449-462, https://doi.org/10.1038/nrn1671
[27] W. Maret, Zinc in Pancreatic Islet Biology, Insulin Sensitivity, and Diabetes, Prev. Nutr. Food Sci. 22 (2017) 1-8, 10.3746/pnf.2017.22.1.1
[28] W. Maret, J. M. Moulis, The Bioinorganic Chemistry of Cadmium in the Context of Its Toxicity, Met. Ions Life Sci. 11 (2013) 1-29, 10.1007/978-94-007-5179-8_1
[29] L. Patrick, Toxic metals and antioxidants: part II. The role of antioxidants in arsenic and cadmium toxicity, Altern Med Rev. 8 (2003) 106-128, https://doi.org/10.1385/BTER:104:1:019
[30] H. Selin, S. D. Van Deveer, Raising Global Standards: Hazardous Substances and E-Waste Management in the European Union, Environment: Science and Policy for Sustainable Development 48 (2006) 6-18, https://doi.org/10.3200/ENVT.48.10.6-18
[31] Cadmium. Geneva, World Health Organization, 1992 (Environmental Health Criteria, No.134).
[32] Z. Kaya, Pollution in *Encyclopedia of Soil Science* (Ed. R. Lal), CRC Press, 2006, 1343-1346.
[33] A. Jensen, F. Bro-Rasmussen, Rev Environ Contam Toxicol., 125 (1992) 101-181, DOI: 10.1007/978-1-4612-2890-5_3
[34] Cadmium, Air Quality Guidelines, 6nd Edition, WHO Regional Office for Europe, Copenhagen, Denmark, 2000.
[35] A. Bencini, V. Lippolis, Probing biologically and environmentally important metal ions with fluorescent chemosensors: Thermodynamic *versus* optical response selectivity in some study cases, Coord. Chem. Rev. 256 (2012) 149-169, https://doi.org/10.1016/j.ccr.2011.05.015
[36] (a) P. Jiang, Z. Guo, Fluorescent detection of zinc in biological systems: recent development on the design of chemosensors and biosensors, Coord. Chem. Rev. 248 (2004) 205-229, https://doi.org/10.1016/j.cct.2003.10.013; (b) F. Qian, C. Zhang, Y. Zhang, W. He, X. Gao, P. Hu, ZGuo, Visible Light Excitable Zn^{2+} Fluorescent Sensor Derived from an Intramolecular Charge Transfer Fluorophore and Its in Vitro and in Vivo Application, J. Am. Chem. Soc. 131 (2009) 1460-1468, https://doi.org/10.1021/ja806489y; (c) K. Hanaoka, Y. Muramatsu, Y. Urano, T. Terai, T. Nagano, Design and synthesis of a highly sensitive off–on fluorescent chemosensor for zinc ions utilizing internal charge transfer, Chem.-Eur. J. 16 (2010) 568-572, https://doi.org/10.1002/chem.200901591; (d) S. Aoki, D. Kagata, M. Shiro, K. Takeda, E. Kimura, Metal chelation-controlled twisted intramolecular charge transfer and its application to fluorescent sensing of metal ions and anions, J. Am. Chem. Soc. 126 (2004) 13377-13390, https://doi.org/10.1021/ja040095v; (e) J. L. Vinkenborg, T. J.

Nicolson, E. A. Bellomo, M. S. Koay, G. A. Rutter, M. Merkx, Genetically encoded FRET sensors to monitor intracellular Zn^{2+} homeostasis, Nat. Methods 6 (2009) 737-740, doi: 10.1038/nmeth.1368; (f) J. Pina, J. Seixas de Melo, F. Pina, C. Lodeiro, J. C. Lima, A. J. Parola, C. Soriano, M. P. Clares, M. T. Albelda, R. Aucejo, Spectroscopy and Coordination Chemistry of a New Bisnaphthalene−Bisphenanthroline Ligand Displaying a Sensing Ability for Metal Cations, Inorg. Chem. 44 (2005) 7449-7458, https://doi.org/10.1021/ic050733q

[37] (a) O. K. Abou-Zied, R. Jimenez, E. H. Z. Thompson, D. P. Millar, F. E. J. Romesberg, Solvent-Dependent Photoinduced Tautomerization of 2-(2′-Hydroxyphenyl)benzoxazole, Phys. Chem. A 106 (2002) 3665-3672, https://doi.org/10.1021/jp013915o; (b) T. Iijima, A. Momotake, Y. Shinohara, T. Sato, Y. Nishimura, T. Arai, Excited-State Intramolecular Proton Transfer of Naphthalene-Fused 2-(2′-Hydroxyaryl)benzazole Family, J. Phys. Chem. A 114 (2010) 1603-1609, https://doi.org/10.1021/jp904370t; (c) S. Rios Vazquez, M. C. Rios Rodriguez, M. Mosquera, F. J. Rodriguez-Prieto, Rotamerism, Tautomerism, and Excited-State Intramolecular Proton Transfer in 2-(4′-*N,N*-Diethylamino-2′-hydroxyphenyl)benzimidazoles: Novel Benzimidazoles Undergoing Excited-State Intramolecular Coupled Proton and Charge Transfer, Phys. Chem. A 112 (2008) 376-387, https://doi.org/10.1021/jp076634a

[38] A. J. Blake, A. Bencini, C. Caltagirone, G. De Filippo, L. S. Dolci, A. Garau, F. Isaia, V. Lippolis, P. Mariani, L. Prodi, M. Montalti, N. Zaccheroni, C. Wilson, A new pyridine-based 12-membered macrocycle functionalised with different fluorescent subunits; coordination chemistry towards Cu^{II}, Zn^{II}, Cd^{II}, Hg^{II}, and Pb^{II}, Dalton Trans. (2004) 2771-2779, https://doi.org/10.1039/B407037B

[39] (a) M. Mameli, M. C. Aragoni, M. Arca, C. Caltagirone, F. Demartin, G. Farruggia, G. De Filippo, F. A. Devillanova, A. Garau, F. Isaia, V. Lippolis, S. Murgia, L. Prodi, A. Pintus, N. Zaccheroni, A Selective, Nontoxic, OFF–ON Fluorescent Molecular Sensor Based on 8-Hydroxyquinoline for Probing Cd^{2+} in Living Cells, Chem. Eur. J. 16 (2010) 919-930, https://doi.org/10.1002/chem.200902005; (b) M. C. Aragoni, M. Arca, A. Bencini, A. Blake, C. Caltagirone, G. De Filippo, F. A. Devillanova, A. Garau, T. Gelbrich, M.B. Hursthouse, F. Isaia, V. Lippolis, M. Mameli, P. Mariani, B. Valtancoli, C. Wilson, Tuning the Selectivity/Specificity of Fluorescent Metal Ion Sensors Based on N_2S_2 Pyridine-Containing Macrocyclic Ligands by Changing the Fluorogenic Subunit: Spectrofluorimetric and Metal Ion Binding Studies, Inorg. Chem. 46 (2007) 4548-4559, https://doi.org/10.1021/ic070169e

[40] M. Shamsipur, M. Sadeghi, K. Alizadeh, A. Bencini, B. Valtancoli, A. Garau, V. Lippolis, Novel fluorimetric bulk optode membrane based on 5,8-bis((5′-chloro-8′-hydroxy-7′-quinolinyl)methyl)-2,11-dithia-5,8-diaza-2,6-pyridinophane for selective detection of lead(II) ions, Talanta 80 (2010) 2023-2033, https://doi.org/10.1016/j.talanta.2009.11.011

[41] M. Shamsipur, M. M. Zahedi, G. De Filippo, V. Lippolis, Development of a novel flow injection liquid–liquid microextraction method for the on-line separation and preconcentration for determination of zinc(II) using 5-(8-hydroxy-2-quinolinylmethyl)-

2,8-dithia-5-aza-2,6-pyridinophane as a sensitive and selective fluorescent chemosensor, Talanta 85 (2011) 687-693, https://doi.org/10.1016/j.talanta.2011.04.049
[42] M. Shamsipur, M. Sadeghi, A. Garau, V. Lippolis, An efficient and selective fluorescent chemical sensor based on 5-(8-hydroxy-2-quinolinylmethyl)-2,8-dithia-5-aza-2,6-pyridinophane as a new fluoroionophore for determination of iron(III) ions. A novel probe for iron speciation, Anal. Chim. Acta 761 (2013) 169-177, https://doi.org/10.1016/j.aca.2012.11.029
[43] C. Bazzicalupi, C. Caltagirone, Z. Cao, Q. Chen, C. Di Natale, A. Garau, V. Lippolis, L. Lvova, H. Liu, I. Lundström, M. C. Mostallino, M. Nieddu, R. Paolesse, L. Prodi, M. Sgarzi, N. Zaccheroni, Multimodal Use of New Coumarin-Based Fluorescent Chemosensors: Towards Highly Selective Optical Sensors for Hg^{2+} Probing, Chem. Eur. J. 19 (2013) 14639-14653, https://doi.org/10.1002/chem.201302090
[44] M. Arca, C. Caltagirone, G. De Filippo, M. Formica, V. Fusi, L. Giorgi, V. Lippolis, L. Prodi, E. Rampazzo, M. A. Scorciapino, M. Sgarzi, N. Zaccheroni, A fluorescent ratiometric nanosized system for the determination of Pd II in water, Chem. Commun. 50 (2014) 15259-15262, https://doi.org/10.1039/C4CC07969H
[45] M. C. Aragoni, M. Arca, A. Bencini, C. Caltagirone, A. Garau, F. Isaia, M. E. Light, V. Lippolis, C. Lodeiro, M. Mameli, R. Montis, M. C. Mostallino, A. Pintus, S. Puccioni, Zn^{2+}/Cd^{2+} optical discrimination by fluorescent chemosensors based on 8-hydroxyquinoline derivatives and sulfur-containing macrocyclic units, Dalton Trans. 42 (2013) 14516-14530, https://doi.org/10.1039/C3DT51292D
[46] M. Formica, G. Ambrosi, V. Fusi, L. Giorgi, M. Arca, A. Garau, A. Pintus, V. Lippolis, Cd^{II}/Zn^{II} discrimination using 2,5-diphenyl[1,3,4]oxadiazole based fluorescent chemosensors, New J. Chem. 42 (2018) 7869-7883, https://doi.org/10.1039/C8NJ00113H
[47] (a) L. Lvova, F. Caroleo, A. Garau, V. Lippolis, L. Giorgi, V. Fusi, N. Zaccheroni, M. Lombardo, L. Prodi, C. Di Natale, R. Paolesse, A fluorescent sensor array based on heteroatomic macrocyclic fluorophores for the detection of polluting species in natural water samples, Front. Chem. (2018) 6:258, https://doi.org/10.3389/fchem.2018.00258; (b) L. Lvova, C. Di Natale, R. Paolesse, L. Giorgi, V. Fusi, A. Garau, V. Lippolis, Photographic detection of cadmium (II) and zinc (II) ions, Procedia Eng. 168 (2016) 346-350
[48] Q. Lin, C. Bao, G. Fan, S. Cheng, H. Liu, Z. Liu, L. Zhu, 7-Amino coumarin based fluorescent phototriggers coupled with nano/bio-conjugated bonds: Synthesis, labeling and photorelease, J. Mater. Chem. 22 (2012) 6680-6688, https://doi.org/10.1039/C2JM30357D
[49] J. Mohanty, H. Pal, A. V. Sapre, Photophysical Properties of 2, 2′-and 4, 4′-Biphenyldiols, Bull. Chem. Soc. Jpn. 72 (1999) 2193-2202, https://doi.org/10.1246/bcsj.72.2193
[50] O. V. Dolomanov, L. J. Bourhis, R. J. Gildea, J. A. K. Howard, H. Puschmann, *OLEX2*: a complete structure solution, refinement and analysis program, J. Appl. Cryst. 42 (2009) 339-341, https://doi.org/10.1107/S0021889808042726

[51] G. M. Sheldrick, Crystal structure refinement with *SHELXL*, Acta Cryst. C27 (2015) 3-8, https://doi.org/10.1107/S2053229614024218
[52] G. M. Sheldrick, *SHELXT* – Integrated space-group and crystal-structure determination, Acta Cryst. A71 (2015) 3-8, doi:10.1107/S2053273314026370
[53] (a) J. E. Kwon, S. Lee, Y. You, K.-H. Baek, K. Ohkubo, J. Cho, S. Fukuzumi, I. Shin, S. Y. Park, W. Nam, Fluorescent Zinc Sensor with Minimized Proton-Induced Interferences: Photophysical Mechanism for Fluorescence Turn-On Response and Detection of Endogenous Free Zinc Ions, Inorg. Chem. 51 (2012) 8760-8774, https://doi.org/10.1021/ic300476e; (b) J. Wang, Q. Chu, X. Liu, C. Wesdemiotis, Y. Pang, Large fluorescence response by alcohol from a bis (benzoxazole)–zinc (II) complex: The role of excited state intramolecular proton transfer, J. Phys. Chem. B 117 (2013) 4127-4133, https://doi.org/10.1021/jp401612u; (c) M. Taki, J. L. Wolford, T. V O'Halloran, Emission ratiometric imaging of intracellular zinc: design of a benzoxazole fluorescent sensor and its application in two-photon microscopy, J. Am. Chem. Soc. 126 (2004) 712-713, https://doi.org/10.1021/ja039073j; (d) J. Wang, Y. Pang, A versatile synthesis of bis [2-(2′-hydroxylphenyl) benzoxazole] derivatives as zinc sensors, RSC Adv. 3 (2013) 10208-10212, DOI: 10.1039/C3RA41080C
[54] J. L. Brisset, Ionic products of water-acetonitrile and methanol-acetonitrile mixtures, Revue Roumaine de Chimie 28 (1983) 941-949
[55] (a) C. Caltagirone, A. Bencini, F. Demartin, F.A. Devillanova, A. Garau, F. Isaia, V. Lippolis, P. Mariani, U. Papke, L. Tei, G. Verani, Redox chemosensors: coordination chemistry towards Cu^{II}, Zn^{II}, Cd^{II}, Hg^{II}, and Pb^{II} of 1-aza-4,10-dithia-7-oxacyclododecane ([12]aneNS$_2$O) and its *N*-ferrocenylmethyl derivative, Dalton Trans. (2003) 901-909, https://doi.org/10.1039/B210806M; (b) M. C. Aragoni, M. Arca, A. Bencini, A. J. Blake, C. Caltagirone, A. Decortes, F. Demartin, F. A. Devillanova, E. Faggi, L. S. Dolci, A. Garau, F. Isaia, V. Lippolis, L. Prodi, C. Wilson, B. Valtancoli, N. Zaccheroni, Coordination chemistry of *N*-aminopropyl pendant arm derivatives of mixed N/S-, and N/S/O-donor macrocycles, and construction of selective fluorimetric chemosensors for heavy metal ions, Dalton Trans. (2005) 2994-3004, https://doi.org/10.1039/B506785E
[56] M. Shamsipur, M. Hosseini, K. Alizadeh, N. Alizadeh, A. Yari, C. Caltagirone, V. Lippolis, Novel fluorimetric bulk optode membrane based on a dansylamidopropyl pendant arm derivative of 1-aza-4,10-dithia-7-oxacyclododecane ([12]aneNS$_2$O) for selective subnanomolar detection of Hg(II) ions, Anal. Chim. Acta 533 (2005) 17-24, https://doi.org/10.1016/j.aca.2004.10.069
[57] A. Legin, A. Rudnitskaya, A. Smirnova, L. Lvova, Yu. Vlasov, Environmental Problems of Chemistry and Technology- Cross Sensitivity of Cation-Selective Film Sensors Based on Polyvinyl Chloride, Rus. J. Appl. Chem. 72 (1999) 114-120
[58] A. L. Page, A. C. Chang, M. El Amamy in Lead, Mercury, Cadmium and Arsenic in the Environment (Eds.: T. C. Hutchinson, K. M. Meema), *International Council for Science (ICSU), Scientific Committee on Problems of the Environment (SCOPE),* John Wiley & Sons Ltd., **1987**.
[59] The critical observation on the performance drawback of the proposed disposable sensor array based on ligands **L1** and **L2** should be done in respect to the analysis of

samples with initial high content of Cd^{2+}, as in Sample 1 in our case. In order to properly assess the analyte by standard addition method, the sample dilution is required, and the degree of a dilution can be evaluated by first an application of a disposable sensor array in non-diluted sample for preliminary estimation of analyte concentration basing on sensing spots luminescence. At the second step, a new disposable sensor should be applied in a properly diluted sample. Another possibility for analysis of samples with high initial concentration of Cd^{2+} is lying in the raise of standard addition concentration. In our experiments, while setting the analytical procedure for Cd^{2+} detection in aqueous soil extracts we have selected the concentrations of cadmium to be spiked in a sample in the range typical for the natural cadmium occurrence (approximately $1.0 \cdot 10^{-5}$ M). As it is appeared during the tests, in Sample 1 the initial value of Cd^{2+} was about two orders of magnitude higher, therefore an addition of a smaller quantity of spiked Cd^{2+} was not possible with a proposed optical sensor array. Unfortunately, the increase of standard addition concentration is not recommended in order to avoid the additional pollution by hazardous Cd^{2+} ions during the analysis.

[60] M. B. McBride, Cadmium Concentration Limits in Agricultural Soils: Weaknesses in USEPA's Risk Assessment and the 503 Rule, Human and Ecological Risk Assessment: An International Journal, 9 (2003) 661-674.

[61] http://www.fao.org/tempref/codex/Meetings/CCCF/CCCF5/cf05_INF.pdf

Tables for

N_2S_2 Pyridinophane-Based Fluorescent Chemosensors for Selective Optical Detection of Cd^{2+} in Soils

Alessandra Garau,[a] Larisa Lvova,*[b] Eleonora Macedi,*[c] Gianluca Ambrosi,[c] M. Carla Aragoni,[a] Massimiliano Arca,[a] Claudia Caltagirone,[a] Simon J. Coles,[d] Mauro Formica,[c] Vieri Fusi,[c] Luca Giorgi,[c] Francesco Isaia,[a] Vito Lippolis,[a] James B. Orton [d] and Roberto Paolesse [c]*

[a]Dipartimento di Scienze Chimiche e Geologiche, Università degli Studi di Cagliari, S.S. 554 Bivio per Sestu, I-09042 Monserrato, Cagliari (Italy). E-mail: agarau@unica.it.

[b]Dipartimento di Scienze e Tecnologie Chimiche, Università di Roma "Tor Vergata", Via della Ricerca Scientifica 1, I-00133, Roma (Italy). E-mail: larisa.lvova@uniroma2.it.

[c]Dipartimento di Scienze Pure e Applicate, Università degli Studi di Urbino "Carlo Bo", via della Stazione 4, I-61029 Urbino (Italy). E-mail: eleonora.macedi@uniurb.it.

[d]UK National Crystallography Service, School of Chemistry, Faculty of Engineering and Physical Sciences, University of Southampton, SO17 1BJ, Southampton (United Kingdom).

Table captions:

Table 1. Compositions of studied membranes.

Table 2. Results of Cd^{2+} content detection in aqueous extracts of soils with **L1**- and **L2**-based optical sensors.

Table 1. Compositions of studied membranes

Membrane	Ligand, 1 wt %	Plasticizer	TpClPBK, wt %
Mb1	**L1**	DOS	-
Mb2	**L1**	oNPOE	-
Mb3	**L1**	oNPOE	2 wt%
Mb4	**L1**	DOS	2 wt%
Mb5	**L1**	DOS	5 wt%
Mb6	**L1**	**TOP**	**5 wt%**
Mb7	**L2**	DOS	-
Mb8	**L2**	oNPOE	-
Mb9	**L2**	oNPOE	2 wt%
Mb10	**L2**	DOS	2 wt%
Mb11[a]	**L2**	DOS	8 wt%
Mb12	**L2**	**TOP**	**2 wt%**

[a] **L2** concentration 3 wt.%

Table 2. Results of Cd^{2+} content detection in aqueous extracts of soils with **L1**- and **L2**-based optical sensors.

Sample		[Cd^{2+}] found in natural soil samples, mg/kg (n = 6)			[Cd^{2+}] determined by sensor array with standard addition method, mM (n = 6)		
		AAS	Mb6	Sensor array	Added	Found	Recovery, %
Sample 1	Airport	0.574	0.511	0.452	0.110	n/a[a]	n/a[a]
Sample 2	Garden	0.010	0.007	0.005	0.110	0.111	100.5
Sample 3	Waste dump	0.030	0.024	0.019	0.110	0.108	98.5

[a]The evaluation was not possible due to the high initial concentration of Cd^{2+} in Sample 1 [59]

Figures for

N_2S_2 Pyridinophane-Based Fluorescent Chemosensors for Selective Optical Detection of Cd^{2+} in Soils

Alessandra Garau,[a] Larisa Lvova,*[b] Eleonora Macedi,*[c] Gianluca Ambrosi,[c] M. Carla Aragoni,[a] Massimiliano Arca,[a] Claudia Caltagirone,[a] Simon J. Coles,[d] Mauro Formica,[c] Vieri Fusi,[c] Luca Giorgi,[c] Francesco Isaia,[a] Vito Lippolis,[a] James B. Orton [d] and Roberto Paolesse [c]*

[a]Dipartimento di Scienze Chimiche e Geologiche, Università degli Studi di Cagliari, S.S. 554 Bivio per Sestu, I-09042 Monserrato, Cagliari (Italy). E-mail: agarau@unica.it.

[b]Dipartimento di Scienze e Tecnologie Chimiche, Università di Roma "Tor Vergata", Via della Ricerca Scientifica 1, I-00133, Roma (Italy). E-mail: larisa.lvova@uniroma2.it.

[c]Dipartimento di Scienze Pure e Applicate, Università degli Studi di Urbino "Carlo Bo", via della Stazione 4, I-61029 Urbino (Italy). E-mail: eleonora.macedi@uniurb.it.

[d]UK National Crystallography Service, School of Chemistry, Faculty of Engineering and Physical Sciences, University of Southampton, SO17 1BJ, Southampton (United Kingdom).

Schemes captions:

Scheme 1 Synthetic pathway adopted for the preparation of **L1.**

Scheme 2 Proposed behavior of **L1** upon addition of Zn^{2+} in DMSO-d_6.

Figures captions:

Fig. 1 Fluorescent chemosensors built using 2,8-dithia-5-aza-2,6-pyridinophane (**L**) as receptor unit with optical selectivity in round brackets.

Fig. 2 Ligands discussed in this paper containing the macrocyclic receptor unit **L** (Scheme 1) together with the numbering scheme for NMR spectral assignments.

Fig. 3 Normalized fluorescence emission at 558 nm of **L1** (MeCN/H_2O 4:1 v/v) upon addition at pH = 7.4 (MOPS buffer $1.0 \cdot 10^{-2}$ M, 25 °C) of 1 equiv. of Zn^{2+}, Cd^{2+}, Cu^{2+}, Co^{2+} (immediately after the addition), Hg^{2+}, Fe^{3+}, K^+, Mg^{2+}, Al^{3+}, Ni^{2+} and Pb^{2+} (after one day) (λ_{ex} = 320 nm). [**L1**] = $5.0 \cdot 10^{-6}$ M.

Fig. 4 Changes in the UV-Vis spectrum of **L1** upon addition of increasing amounts of Zn^{2+} (a), inset: corresponding absorbance at 436 nm *versus* molar ratio plot; changes in the emission

spectrum of **L1** upon addition of increasing amounts of Zn^{2+} (b), inset: corresponding normalized fluorescent intensity at 558 nm *versus* molar ratio plot ([**L1**] = 5.0· 10^{-6} M, MeCN/H_2O (4:1 v/v), pH = 7.4, MOPS buffer 1.0·10^{-2} M, 25 °C, λ_{ex} = 320 nm. Time elapsed between additions: 5 minutes).

Fig. 5 Normalized fluorescence emission intensity of **L1** for the ion competition study performed by adding Zn^{2+} to a solution containing an equimolar mixture of **L1** and M^{n+} (M^{n+} = Cd^{2+}, Co^{2+}, Cu^{2+}, Fe^{3+}, Hg^{2+}, K^+, Mg^{2+}, Al^{3+}, Ni^{2+} and Pb^{2+}) ([**L1**] = 5.0·10^{-6} M, MeCN/H_2O (4:1 v/v), pH 7.4, MOPS buffer 1.0·10^{-2} M, 25 °C, λ_{ex} = 320 nm, λ_{em} = 558 nm). [**L1**] = 5.0· 10^{-6} M.

Fig. 6 Normalized fluorescence emission of **L2** (MeCN/H_2O 4:1 v/v) upon addition at pH = 7.4 (MOPS buffer 1.0·10^{-2} M) of 1 equiv. of Cd^{2+}, Co^{2+}, Cu^{2+}, Fe^{3+}, Hg^{2+}, K^+, Mg^{2+}, Al^{3+}, Ni^{2+}, Zn^{2+} and Pb^{2+} (λ_{ex} = 340 nm, λ_{em} = 433 nm). [**L2**] = 2.5·10^{-5} M.

Fig. 7 Changes in the UV-Vis spectrum of **L2** upon addition of increasing amounts of Cd^{2+} (a), inset: corresponding absorbance at 324 nm *versus* molar ratio plot; changes in the emission spectrum of **L2** upon addition of increasing amounts of Cd^{2+} (b), inset: corresponding normalized fluorescent intensity *versus* molar ratio ([**L2**] = 2.5·10^{-5} M, MeCN/H_2O (4:1 v/v), pH = 7.4 MOPS buffer 1.0·10^{-2} M, 25 °C, λ_{ex} = 340 nm, λ_{em} = 433 nm).

Fig. 8 Normalized fluorescence emission intensity of **L2** for the ion competition study performed by adding 5 equivs. of M^{n+} (M^{n+} = Zn^{2+}, Co^{2+}, Cu^{2+}, Fe^{3+}, Hg^{2+}, K^+, Mg^{2+}, Al^{3+}, Ni^{2+} and Pb^{2+}) to an equimolar solution of **L2** and Cd^{2+} ([**L2**] = 2.4·10^{-5} M, MeCN/H_2O (4:1 v/v), pH 7.4 MOPS buffer 1.0·10^{-2} M, 25 °C, λ_{ex} = 340 nm, λ_{em} = 433 nm). [**L2**] = 2.5·10^{-5} M.

Fig. 9 ^{1}H NMR spectra in DMSO-d_6 of free **L1** (a), upon sequential addition of 1 equiv. of Zn^{2+} ion (as perchlorate salt) (b), and 1 equiv. of Bu_4NOH (c). Black circles: protonated **L1**, (H**L1**)$^+$, signals; black stars: Zn^{2+} complex ([Zn(H_{-1}**L1**)]$^+$) signals. For the numbering scheme see Fig. 2.

Fig. 10 ^{1}H NMR spectra of free **L2** and in the presence of 1 equiv. of Cd^{2+} ion as nitrate salt in $CD_3CN/CDCl_3$ (7:3 v/v). For the numbering scheme see Fig. 2 (* $CDCl_3$, ** impurities).

Fig. 11 Asymmetric unit of [Cd**L2**(NO_3)$_2$] (**1**) with the numbering scheme adopted. Thermal ellipsoids are drawn at 50% probability level. Selected bond distances and angles: Cd1–N1 = 2.419(2), Cd1–N2 = 2.532(2), Cd1–S1 = 2.6555(4), Cd1–S2 = 2.6450(4), Cd1–O8 = 2.420(2), Cd1–O14 = 2.584(2), Cd1–O11 = 2.359(2) Å; N1–Cd1–N2 = 81.20(5), N1–Cd1–S1 = 75.98(3), N1–Cd1–S2 = 77.50(3), N2–Cd1–S1 = 79.33(3), N2–Cd1–S2 = 77.16(3), S1–Cd1–S2 = 146.784(14)^o.

Fig. 12 The photogram of PT response of **L1**- and **L2**-based optodes in binary solutions of Cd^{2+} and Zn^{2+} ions. Membranes doped with ligand **L1** were conditioned in 0.01 M TRIS at pH 8.6 for 15 min, then the measurements were performed in 0.01 M HEPES buffer at pH 7.5 and LED illumination at λ_{ex} = 380 nm.

Fig. 13 Fluorescence response changes of membranes Mb4-Mb6 and Mb10-Mb12 prepared with **L1** and **L2**, respectively, toward several cations in their individual solutions evaluated with PT at λ_{ex} = 380 nm LED illumination in 0.01 M HEPES buffer at pH 7.5.

Fig. 14 The photogram of Cd^{2+} assessment in soils with developed **L1**- and **L2**-based optodes, Mb6 and Mb12, respectively, in 0.01 M HEPES at pH 7.5 background solution upon LED illumination at λ_{ex} = 380 nm.

Fig. 15 (A) PLS1 calibration curve employed for Cd^{2+} ions content analysis with **L1**- and **L2**-based optical sensors array; (B) PCA scores and loadings plot of the fluorescent sensor array responses in Cd^{2+} calibration solutions in the concentration range from $1.0 \cdot 10^{-7}$ to $1.0 \cdot 10^{-2}$ M and in analyzed aqueous extracts of soil samples. In graph B, R and G tags for sensors loadings correspond to the optodes optical intensity variations in the red and green channels, respectively.

Scheme 1.

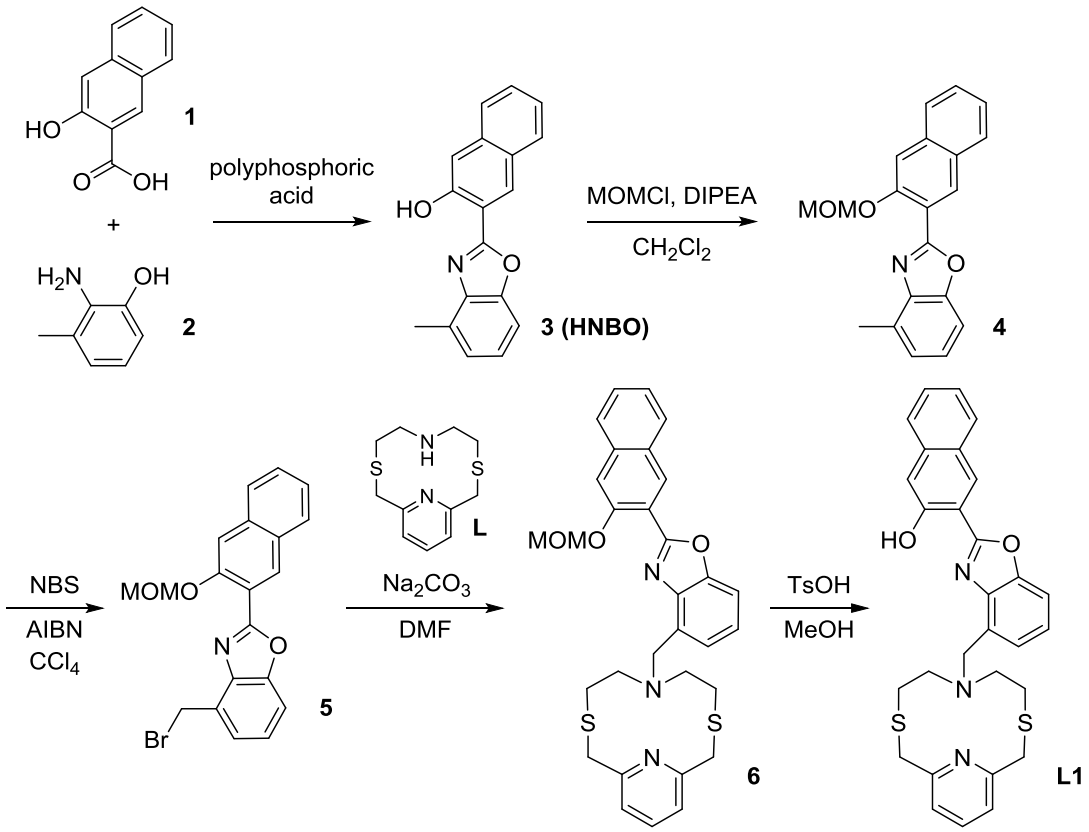

Scheme 1 Synthetic pathway adopted for the preparation of **L1.**

Scheme 2.

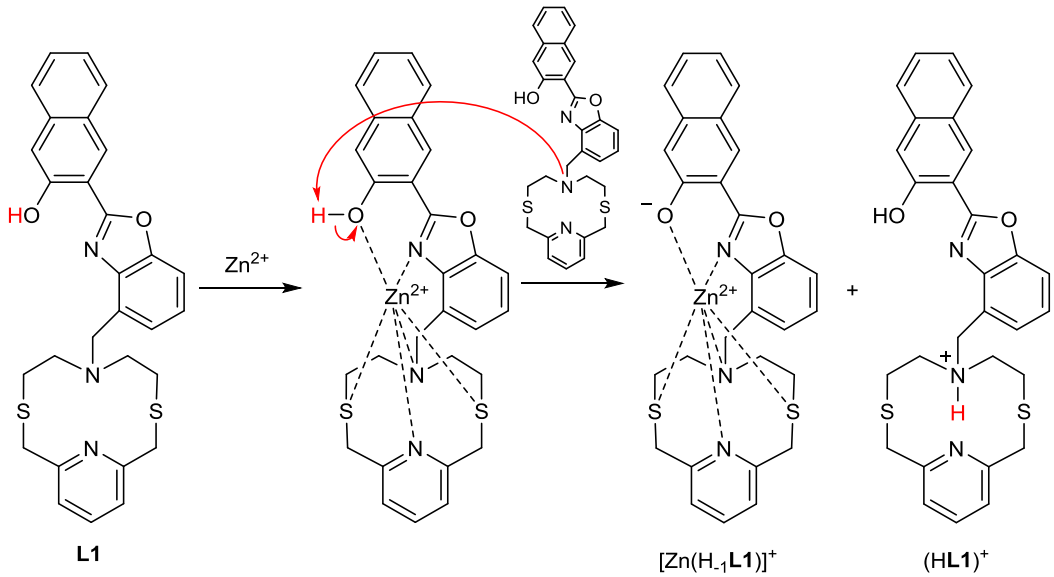

Scheme 2 Proposed behavior of **L1** upon addition of Zn^{2+} in DMSO-d_6.

Figure 1.

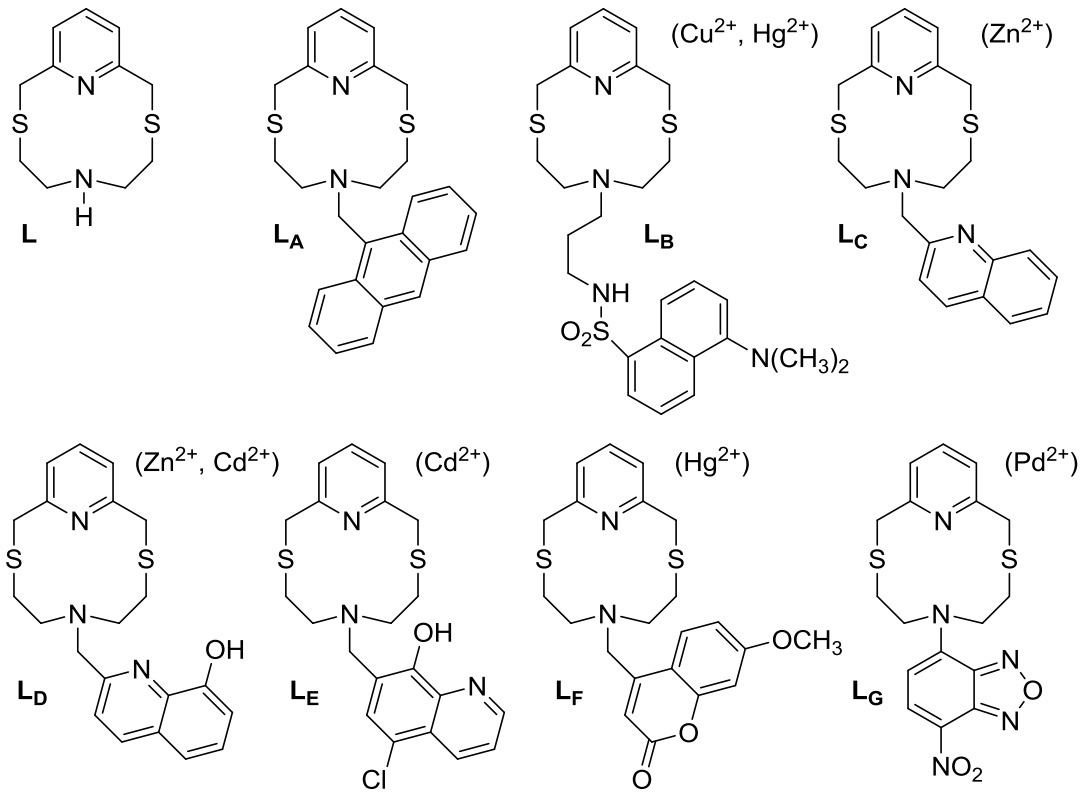

Fig. 1 Fluorescent chemosensors built using 2,8-dithia-5-aza-2,6-pyridinophane (**L**) as receptor unit with optical selectivity in round brackets.

Figure 2.

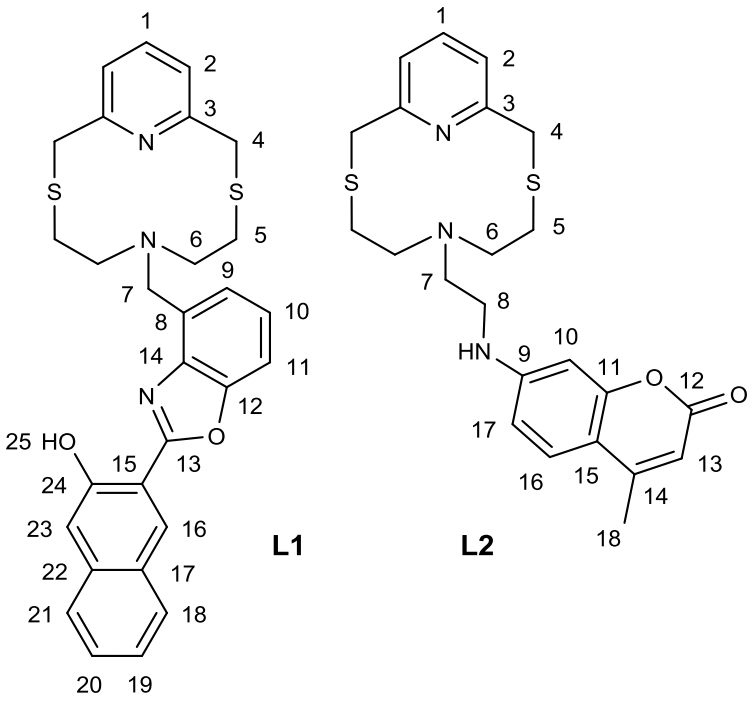

Fig. 2 Ligands discussed in this paper containing the macrocyclic receptor unit **L** (Scheme 1) together with the numbering scheme for NMR spectral assignments.

Figure 3.

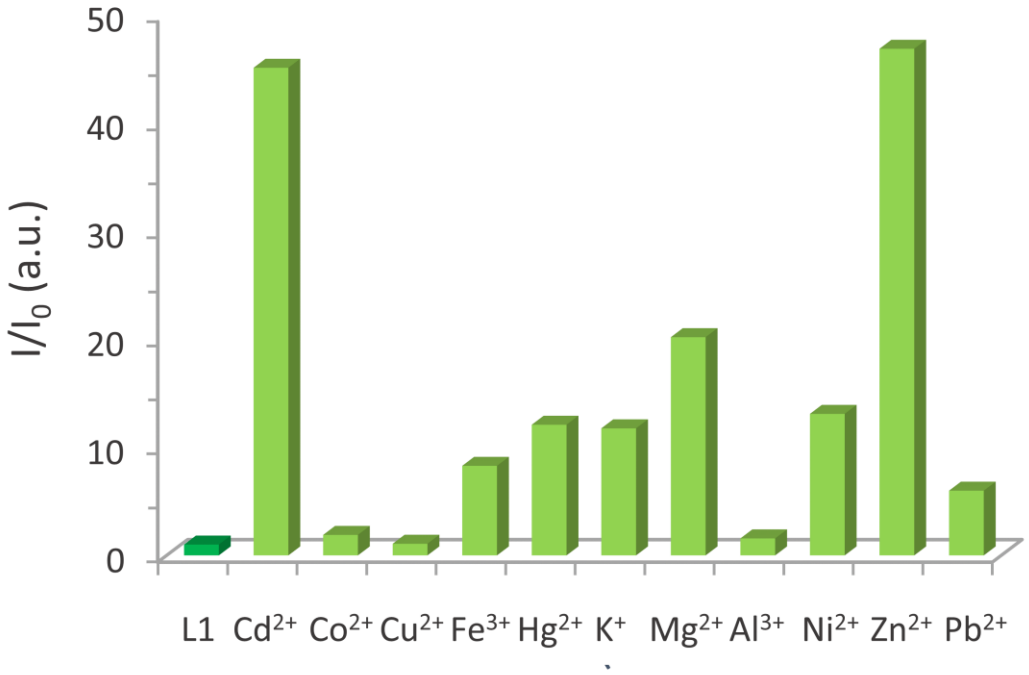

Fig. 3 Normalized fluorescence emission at 558 nm of **L1** (MeCN/H_2O 4:1 v/v) upon addition at pH = 7.4 (MOPS buffer $1.0 \cdot 10^{-2}$ M, 25 °C) of 1 equiv. of Zn^{2+}, Cd^{2+}, Cu^{2+}, Co^{2+} (immediately after the addition), Hg^{2+}, Fe^{3+}, K^{+}, Mg^{2+}, Al^{3+}, Ni^{2+} and Pb^{2+} (after one day) (λ_{ex} = 320 nm). [**L1**] = $5.0 \cdot 10^{-6}$ M.

Figure 4.

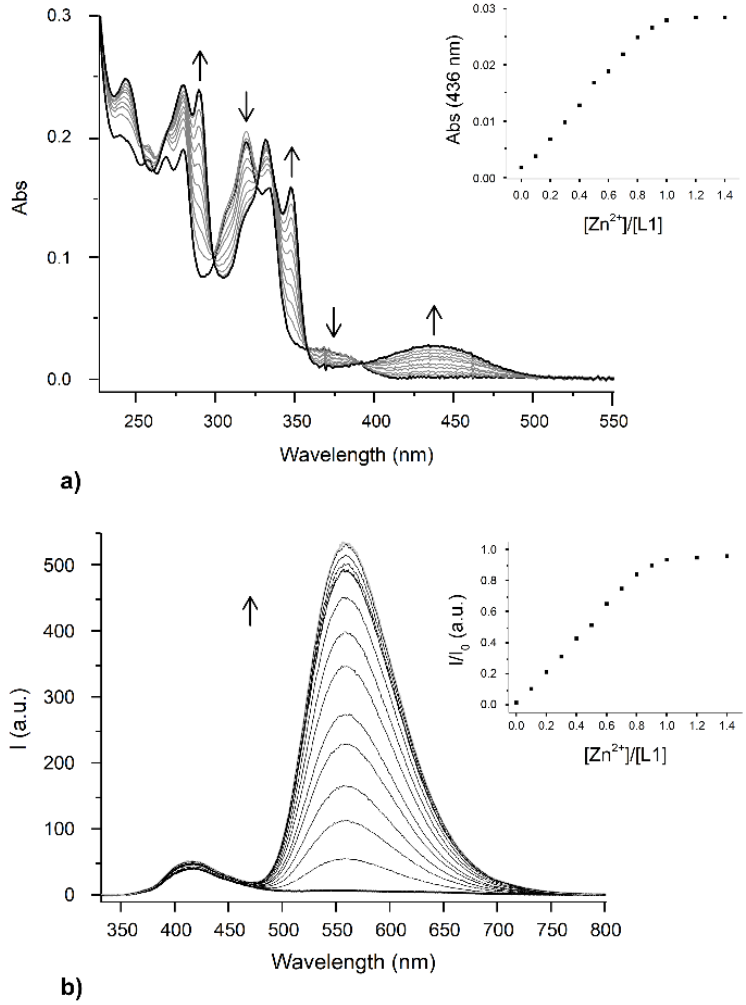

Fig. 4 Changes in the UV-Vis spectrum of **L1** upon addition of increasing amounts of Zn^{2+} (a), inset: corresponding absorbance at 436 nm *versus* molar ratio plot; changes in the emission spectrum of **L1** upon addition of increasing amounts of Zn^{2+} (b), inset: corresponding normalized fluorescent intensity at 558 nm *versus* molar ratio plot ([**L1**] = 5.0· 10^{-6} M, MeCN/H_2O (4:1 v/v), pH = 7.4, MOPS buffer 1.0·10^{-2} M, 25 °C, λ_{ex} = 320 nm. Time elapsed between additions: 5 minutes).

Figure 5.

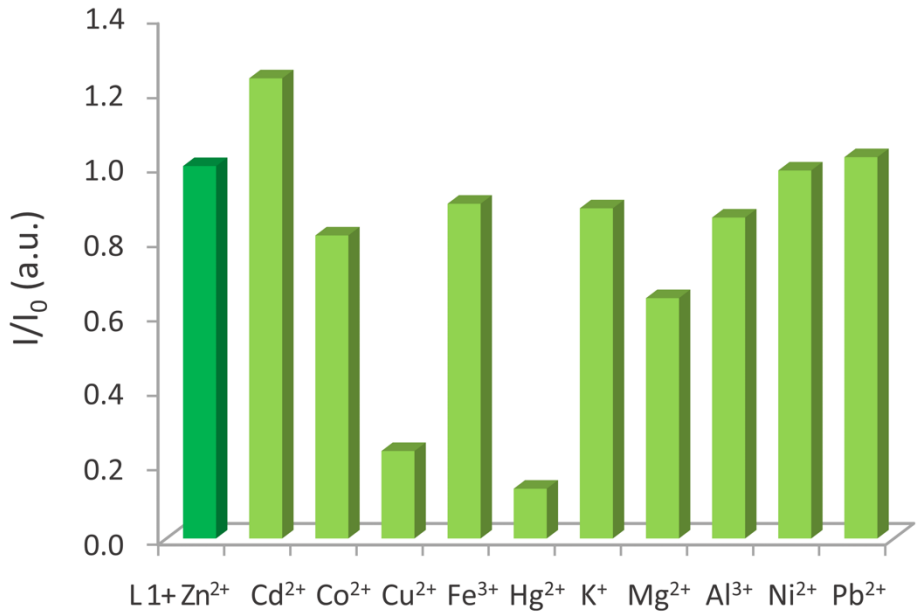

Fig. 5 Normalized fluorescence emission intensity of **L1** for the ion competition study performed by adding Zn^{2+} to a solution containing an equimolar mixture of **L1** and M^{n+} (M^{n+} = Cd^{2+}, Co^{2+}, Cu^{2+}, Fe^{3+}, Hg^{2+}, K^{+}, Mg^{2+}, Al^{3+}, Ni^{2+} and Pb^{2+}) ([**L1**] = $5.0 \cdot 10^{-6}$ M, MeCN/H_2O (4:1 v/v), pH 7.4, MOPS buffer $1.0 \cdot 10^{-2}$ M, 25 °C, λ_{ex} = 320 nm, λ_{em} = 558 nm). [**L1**] = $5.0 \cdot 10^{-6}$ M.

Figure 6.

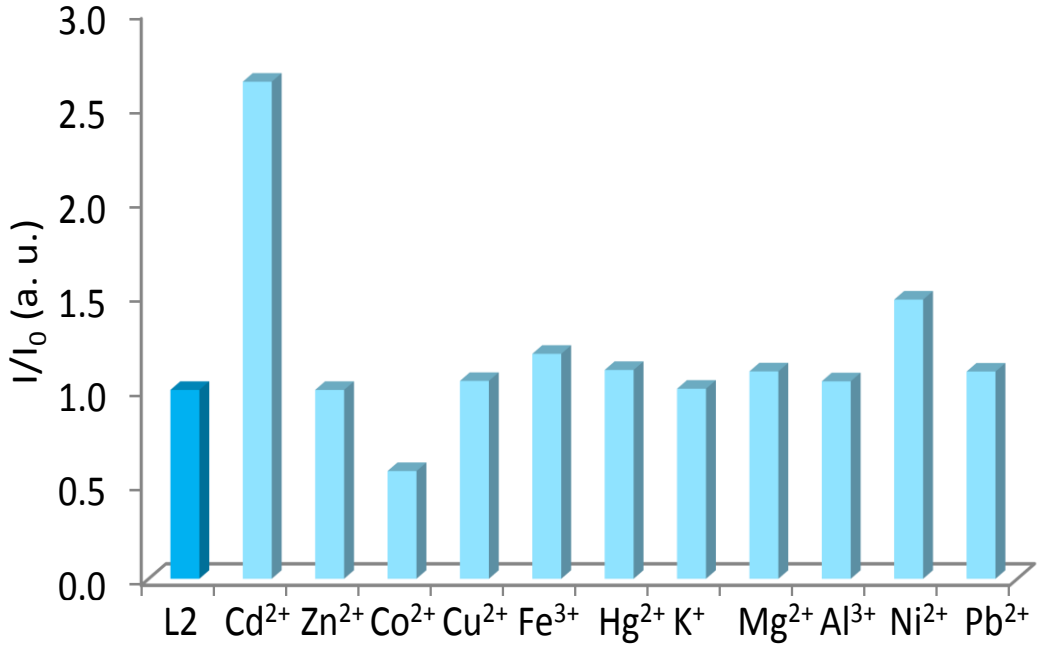

Fig. 6 Normalized fluorescence emission of **L2** (MeCN/H_2O 4:1 v/v) upon addition at pH = 7.4 (MOPS buffer $1.0 \cdot 10^{-2}$ M) of 1 equiv. of Cd^{2+}, Co^{2+}, Cu^{2+}, Fe^{3+}, Hg^{2+}, K^{+}, Mg^{2+}, Al^{3+}, Ni^{2+}, Zn^{2+} and Pb^{2+} (λ_{ex} = 340 nm, λ_{em} = 433 nm). [**L2**] = $2.5 \cdot 10^{-5}$ M.

Figure 7.

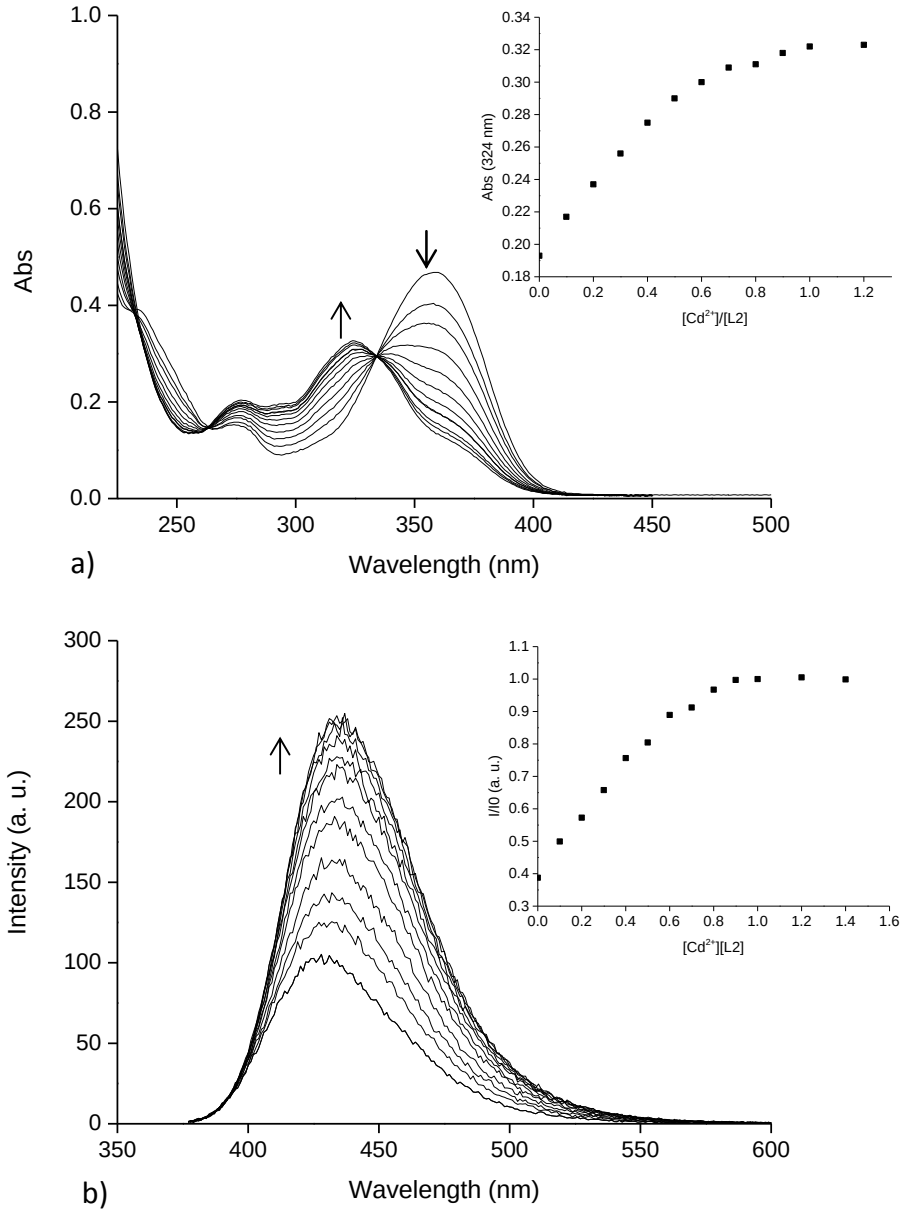

Fig. 7 Changes in the UV-Vis spectrum of **L2** upon addition of increasing amounts of Cd^{2+} (a), inset: corresponding absorbance at 324 nm *versus* molar ratio plot; changes in the emission spectrum of **L2** upon addition of increasing amounts of Cd^{2+} (b), inset: corresponding normalized fluorescent intensity *versus* molar ratio ([**L2**] = $2.5 \cdot 10^{-5}$ M, MeCN/H_2O (4:1 v/v), pH = 7.4 MOPS buffer $1.0 \cdot 10^{-2}$ M, 25 °C, λ_{ex} = 340 nm, λ_{em} = 433 nm).

Figure 8.

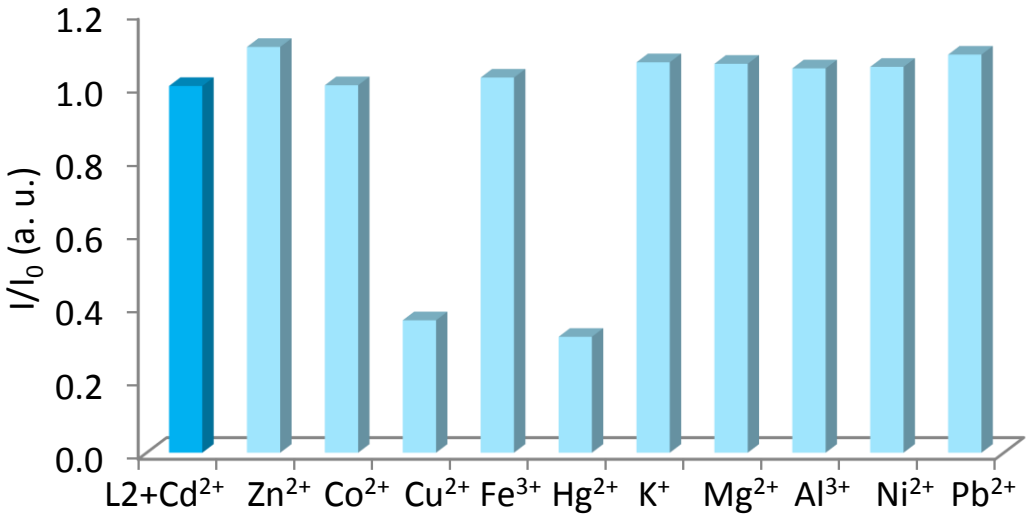

Fig. 8 Normalized fluorescence emission intensity of **L2** for the ion competition study performed by adding 5 equivs. of M^{n+} (M^{n+} = Zn^{2+}, Co^{2+}, Cu^{2+}, Fe^{3+}, Hg^{2+}, K^{+}, Mg^{2+}, Al^{3+}, Ni^{2+} and Pb^{2+}) to an equimolar solution of **L2** and Cd^{2+} ([**L2**] = $2.4\cdot10^{-5}$ M, MeCN/H_2O (4:1 v/v), pH 7.4 MOPS buffer $1.0\cdot10^{-2}$ M, 25 °C, λ_{ex} = 340 nm, λ_{em} = 433 nm). [**L2**] = $2.5\cdot10^{-5}$ M.

Figure 9.

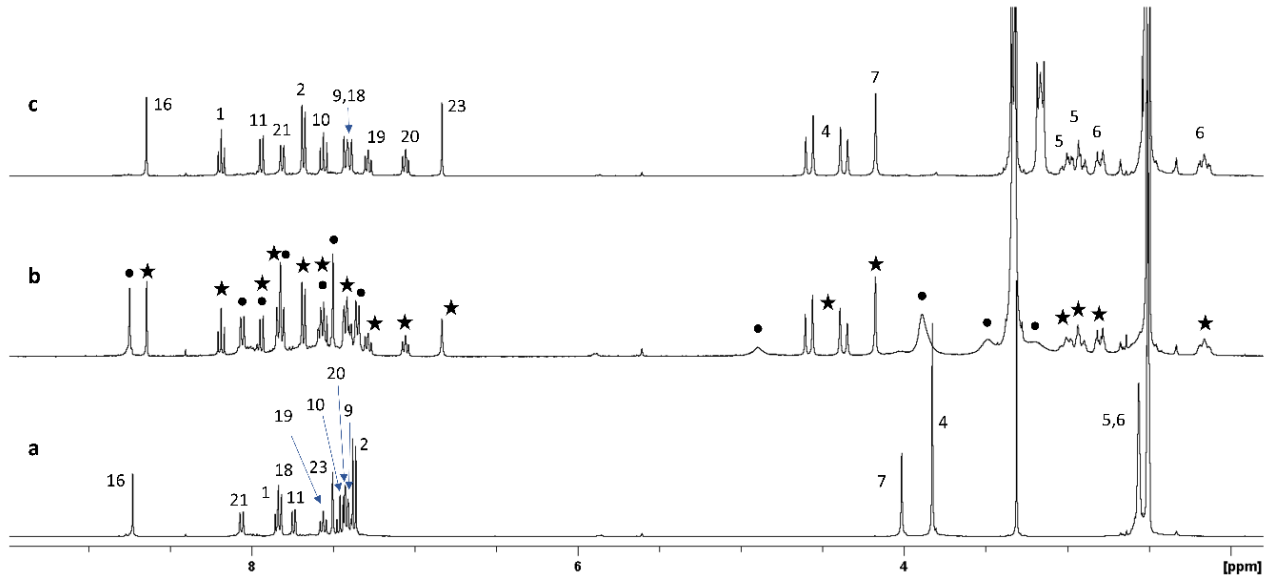

Fig. 9 ^{1}H NMR spectra in DMSO-d_6 of free **L1** (a), upon sequential addition of 1 equiv. of Zn^{2+} ion (as perchlorate salt) (b), and 1 equiv. of Bu_4NOH (c). Black circles: protonated **L1**, (H**L1**)$^{+}$, signals; black stars: Zn^{2+} complex ([Zn(H_{-1}**L1**)]$^{+}$) signals. For the numbering scheme see Fig. 2.

Figure 10.

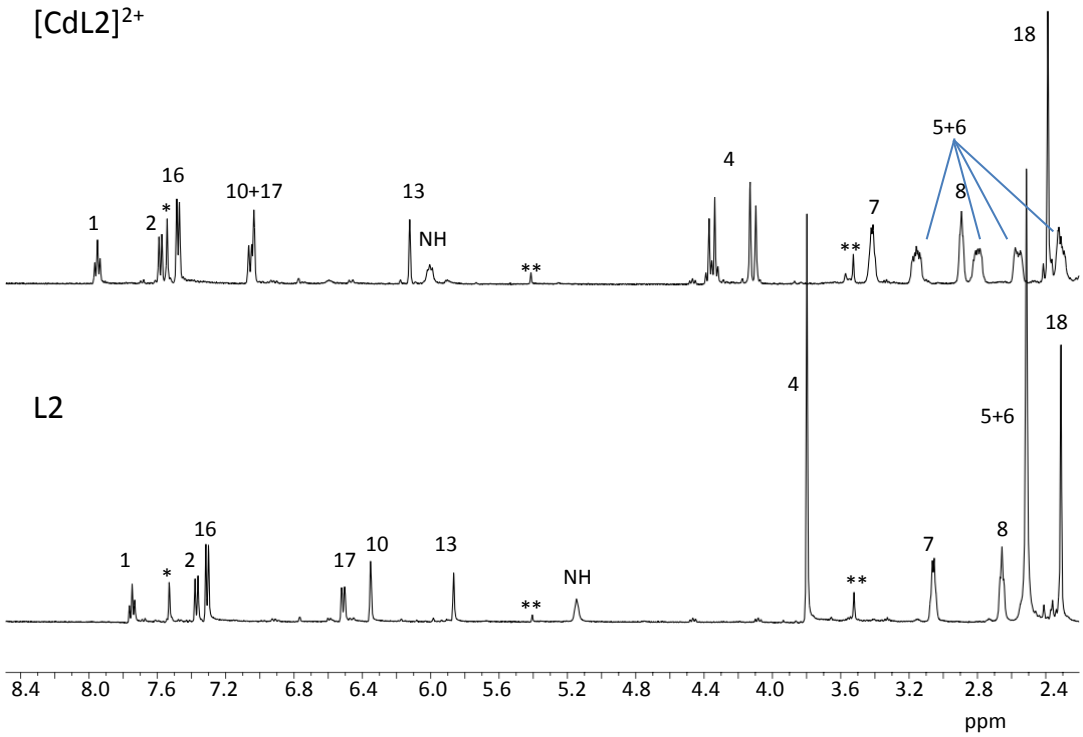

Fig. 10 ^{1}H NMR spectra of free **L2** and in the presence of 1 equiv. of Cd^{2+} ion as nitrate salt in $CD_3CN/CDCl_3$ (7:3 v/v). For the numbering scheme see Fig. 2 (* $CDCl_3$, ** impurities).

Figure 11.

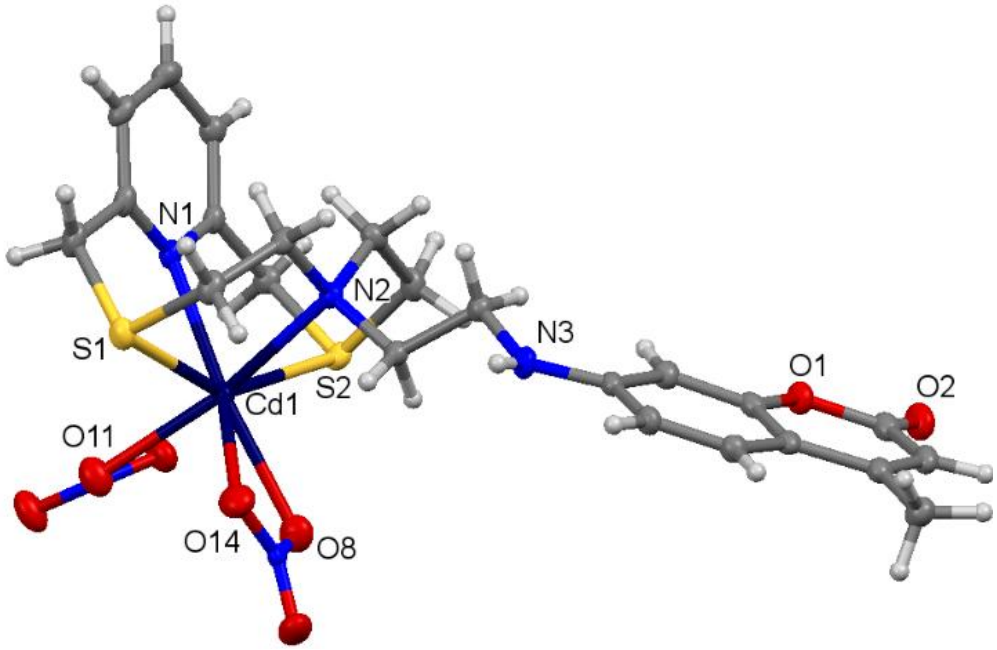

Fig. 11 Asymmetric unit of [Cd**L2**$(NO_3)_2$] (**1**) with the numbering scheme adopted. Thermal ellipsoids are drawn at 50% probability level. Selected bond distances and angles: Cd1–N1 = 2.419(2), Cd1–N2 = 2.532(2), Cd1–S1 = 2.6555(4), Cd1–S2 = 2.6450(4), Cd1–O8 = 2.420(2), Cd1–O14 = 2.584(2), Cd1–O11 = 2.359(2) Å; N1–Cd1–N2 = 81.20(5), N1–Cd1–S1 = 75.98(3), N1–Cd1–S2 = 77.50(3), N2–Cd1–S1 = 79.33(3), N2–Cd1–S2 = 77.16(3), S1–Cd1–S2 = 146.784(14)^{o}.

Figure 12.

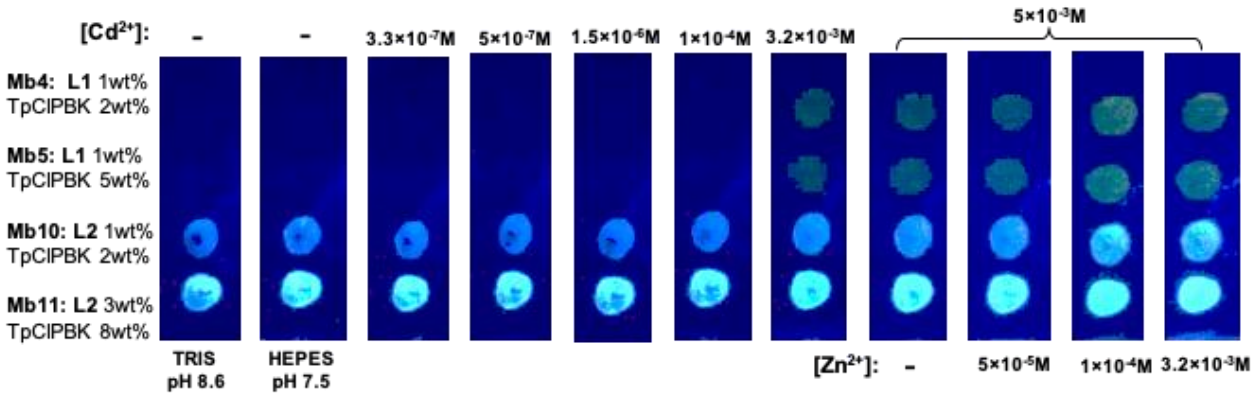

Fig. 12 The photogram of PT response of **L1**- and **L2**-based optodes in binary solutions of Cd^{2+} and Zn^{2+} ions. Membranes doped with ligand **L1** were conditioned in 0.01 M TRIS at pH 8.6 for 15 min, then the measurements were performed in 0.01 M HEPES buffer at pH 7.5 and LED illumination at λ_{ex} = 380 nm.

Figure 13.

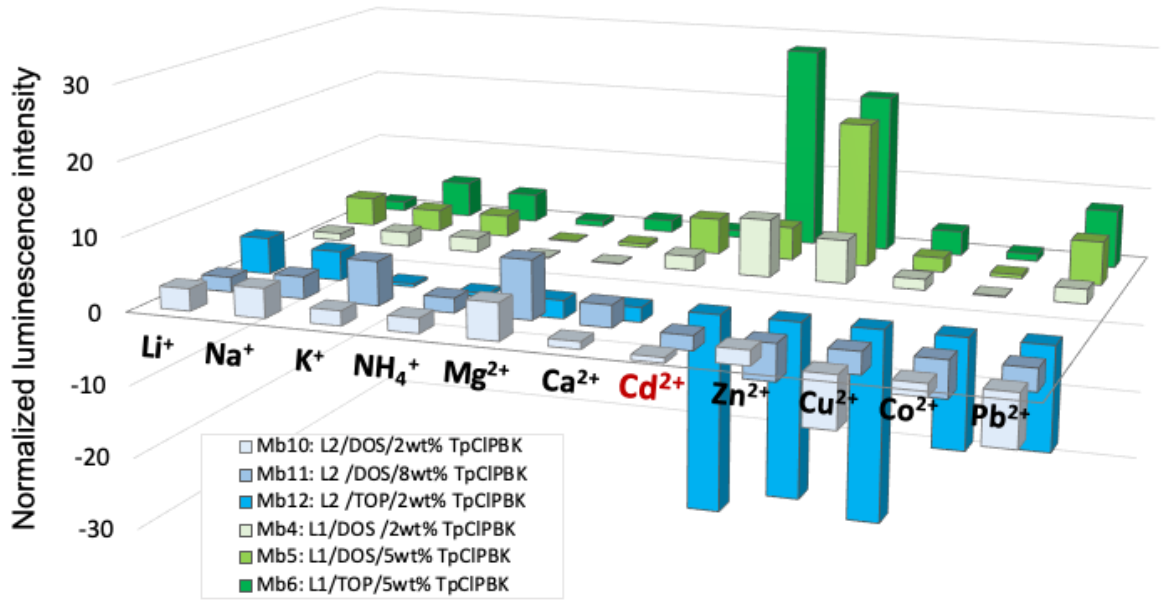

Fig. 13 Fluorescence response changes of membranes Mb4-Mb6 and Mb10-Mb12 prepared with **L1** and **L2**, respectively, toward several cations in their individual solutions evaluated with PT at λ_{ex} = 380 nm LED illumination in 0.01 M HEPES buffer at pH 7.5.

Figure 14.

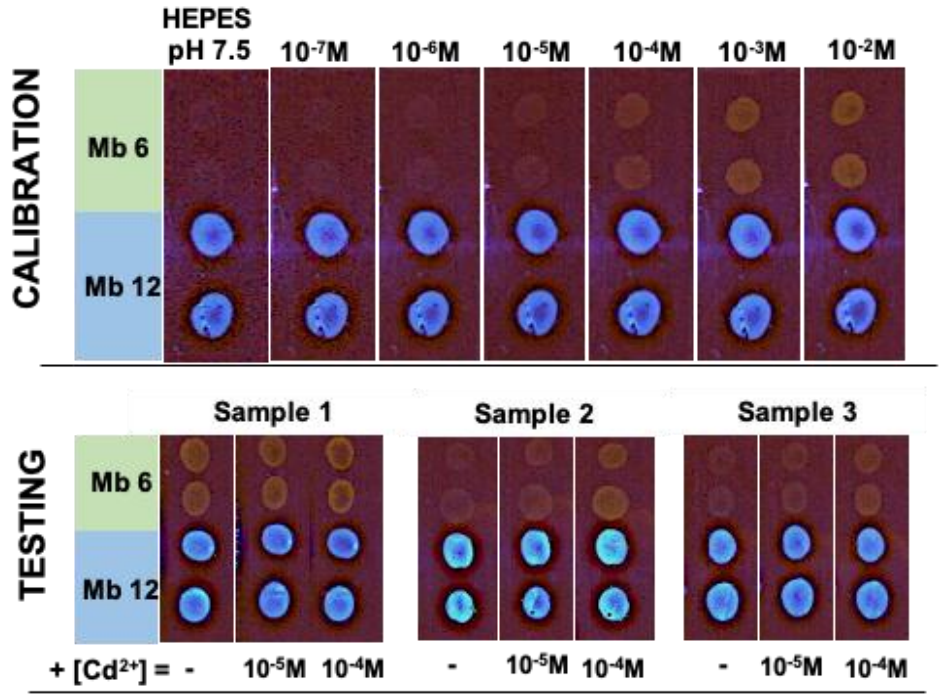

Fig. 14 The photogram of Cd^{2+} assessment in soils with developed **L1**- and **L2**-based optodes, Mb6 and Mb12, respectively, in 0.01 M HEPES at pH 7.5 background solution upon LED illumination at λ_{ex} = 380 nm.

Figure 15.

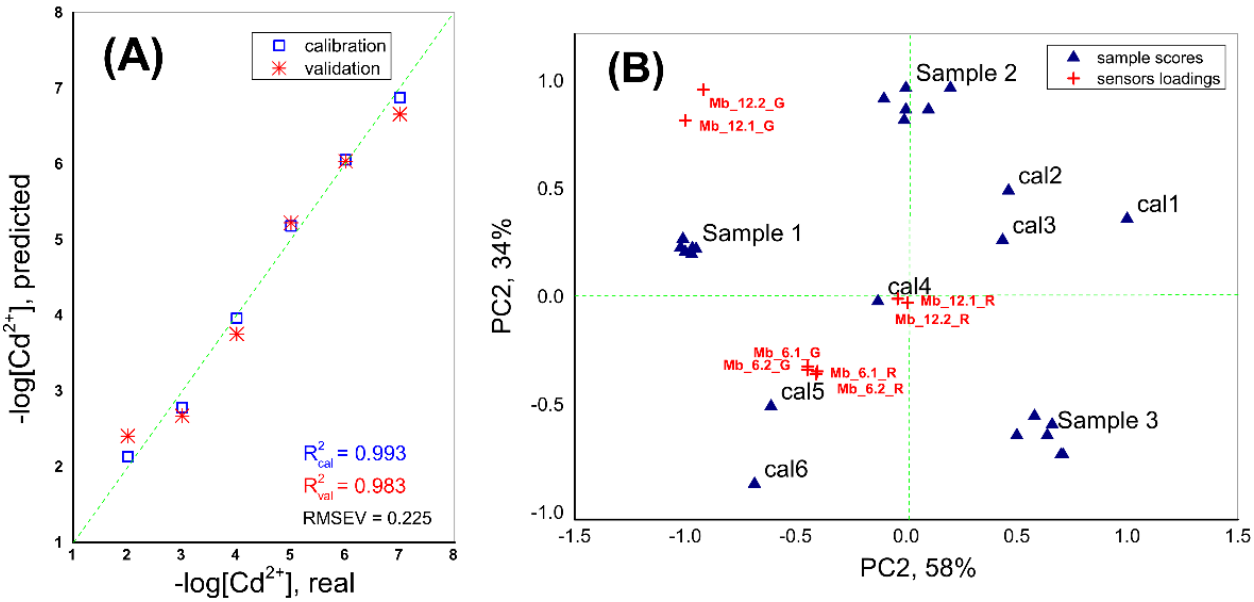

Fig. 15 (A) PLS1 calibration curve employed for Cd^{2+} ions content analysis with **L1**- and **L2**-based optical sensors array; (B) PCA scores and loadings plot of the fluorescent sensor array responses in Cd^{2+} calibration solutions in the concentration range from $1.0 \cdot 10^{-7}$ to $1.0 \cdot 10^{-2}$ M and in analyzed aqueous extracts of soil samples. In graph B, R and G tags for sensors loadings correspond to the optodes optical intensity variations in the red and green channels, respectively.

Supplementary Material

Click here to download Supplementary Material: ESI_Cd_SNB.doc

Supplementary Interactive Plot Data (CSV)

Click here to download Supplementary Interactive Plot Data (CSV): checkCIFstructure_Cd_SNB.pdf

Highlights for

N_2S_2 Pyridinophane-Based Fluorescent Chemosensors for Selective Optical Detection of Cd^{2+} in Soils

Alessandra Garau,[a] Larisa Lvova,*[b] Eleonora Macedi,*[c] Gianluca Ambrosi,[c] M. Carla Aragoni,[a] Massimiliano Arca,[a] Claudia Caltagirone,[a] Simon J. Coles,[d] Mauro Formica,[c] Vieri Fusi,[c] Luca Giorgi,[c] Francesco Isaia,[a] Vito Lippolis,[a] James B. Orton [d] and Roberto Paolesse [c]*

[a]Dipartimento di Scienze Chimiche e Geologiche, Università degli Studi di Cagliari, S.S. 554 Bivio per Sestu, I-09042 Monserrato, Cagliari (Italy). E-mail: agarau@unica.it.

[b]Dipartimento di Scienze e Tecnologie Chimiche, Università di Roma "Tor Vergata", Via della Ricerca Scientifica 1, I-00133, Roma (Italy). E-mail: larisa.lvova@uniroma2.it.

[c]Dipartimento di Scienze Pure e Applicate, Università degli Studi di Urbino "Carlo Bo", via della Stazione 4, I-61029 Urbino (Italy). E-mail: eleonora.macedi@uniurb.it.

[d]UK National Crystallography Service, School of Chemistry, Faculty of Engineering and Physical Sciences, University of Southampton, SO17 1BJ, Southampton (United Kingdom).

- ✓ A complementary synthetic strategy was employed to obtain **L1** and **L2** chemosensors.
- ✓ Spectrophotometric, spectrofluorimetric and NMR studies on ligand interactions with heavy metal ions were performed.
- ✓ **L1** showed the highest optical sensitivity for Zn^{2+} and Cd^{2+} ions, while **L2** was found to be Cd^{2+}-selective.
- ✓ Fluorescent optodes based on **L1** and **L2** inside PVC polymeric membranes for Cd^{2+} ion detection in real samples were developed.
- ✓ The optodes were used for Cd^{2+} assessment in soils; the obtained results were in a good agreement to a standard AAS method.

Cover letter

TOR VERGATA
UNIVERSITÀ DEGLI STUDI DI ROMA
Dipartimento di Scienze e Tecnologie Chimiche
Via delle Ricerca Scientifica - 00133 Roma
Tel. +390672594755 – Fax +390672594328

UNIVERSITA' DEGLI STUDI DI CAGLIARI
DIPARTIMENTO DI SCIENZE CHIMICHE E GEOLOGICHE
Cittadella Universitaria – 09042 Monserrato – Cagliari
Tel 0706754450

1506 UNIVERSITÀ DEGLI STUDI DI URBINO CARLO BO
DISPEA DIPARTIMENTO DI SCIENZE PURE E APPLICATE

27th July, 2020

Dear Editor,

We are delighted to submit our paper entitled:

N_2S_2 Pyridinophane-Based Fluorescent Chemosensors for Selective Optical Detection of Cd^{2+} in Soils

by A. Garau, L. Lvova, E. Macedi, G. Ambrosi, M. C. Aragoni, M. Arca, C. Caltagirone, S. J. Coles, M. Formica, V. Fusi, L. Giorgi, F. Isaia, V. Lippolis, J. B. Orton and R. Paolesse

which we would like to be considered for publication in ***Sensors and Actuators B: Chemical.***

In the present work the synthesis, coordination properties in solution and application in optical chemical sensors towards Zn^{2+} and Cd^{2+} of the ligands **L1** and **L2,** containing the macrocycle 2,8-dithia-5-aza-2,6-pyridinophane (**L**) as a receptor unit and the 2-(2′-Hydroxy-3′-naphthyl)-4-methylbenzoxazole (HNBO) or the 7-(2-ethylamino)-4-methylcoumarin chromophores as pendant arms, respectively, have been reported. Spectrophotometric and spectrofluorimetric investigations together with NMR measurements allowed to get a deeper insight into the nature of the complexes formed by **L1** and **L2** with Zn^{2+} and Cd^{2+} ions, and on the transduction mechanisms responsible for the optical responses of the two ligands observed in the presence of these metal ions.

Being the result of a collaboration between several research groups specialized in chemical sensors development and multisensory analysis, this work demonstrates the efficacy of the "complementary synthetic strategy" in reaching an optical selectivity towards heavy metal ions. According to the suggested strategy, different fluorogenic fragments are attached to a predefined receptor unit through an appropriate linker, and the resulting "synergic cooperation" between the receptor and signaling units of the obtained ligand determine the optical selectivity of such conjugated chemosensor. The optical selectivity has allowed for the preparation of fluorescent sensitive materials based on PVC polymeric membranes for the quantitative determination of Cd^{2+} ion in real samples. The new sensor devices have been successfully used in a sensor array for the quantitative determination of samples of environmental importance such as soils of different provenance, once combined with the Photoassisted Technique (PT) for signal acquisition. The obtained results were in good agreement with a standard AAS method employed for Cd^{2+} ion analysis in tested soils.

As this work is quite multidisciplinary, different expertise from different research groups have been involved:

- Synthesis and solution studies on **L1**: Gianluca Ambrosi, Luca Giorgi, Eleonora Macedi;
- ^{1}H- and ^{13}C NMR studies on **L1**: Mauro Formica;
- Synthesis and solution studies on **L2**: Alessandra Garau, Claudia Caltagirone, M. Carla Aragoni;
- ^{1}H- and ^{13}C NMR studies on **L2**: Alessandra Garau, Francesco Isaia, Massimiliano Arca;
- Development and study of polymeric membrane optodes: Larisa Lvova, Roberto Paolesse;
- Crystallographic studies: James B. Orton, Simon J. Coles;

- Supervision and writing of the manuscript: Alessandra Garau, Larisa Lvova, Eleonora Macedi, Vieri Fusi, Vito Lippolis, Roberto Paolesse.

Due to the collaboration between several research groups, three co-corresponding authors are listed in this work, namely A. Garau, L. Lvova, E. Macedi.

In our opinion, our research could be of interest to scientists working in the area of optical chemosensors and multisensor systems development and application: for these reasons, we believe it is suitable for publication in ***Sensors and Actuators B: Chemical.***

Please, do not hesitate to contact us if you require any further information or data.

Many thanks for your time and consideration.

Best regards

Alessandra Garau
Larisa Lvova
Eleonora Macedi

Graphical Abstract for

N_2S_2 Pyridinophane-Based Fluorescent Chemosensors for Selective Optical Detection of Cd^{2+} in Soils

Alessandra Garau,[a] Larisa Lvova,*[b] Eleonora Macedi,*[c] Gianluca Ambrosi,[c] M. Carla Aragoni,[a] Massimiliano Arca,[a] Claudia Caltagirone,[a] Simon J. Coles,[d] Mauro Formica,[c] Vieri Fusi,[c] Luca Giorgi,[c] Francesco Isaia,[a] Vito Lippolis,[a] James B. Orton [d] and Roberto Paolesse [c]*

[a]Dipartimento di Scienze Chimiche e Geologiche, Università degli Studi di Cagliari, S.S. 554 Bivio per Sestu, I-09042 Monserrato, Cagliari (Italy). E-mail: agarau@unica.it.

[b]Dipartimento di Scienze e Tecnologie Chimiche, Università di Roma "Tor Vergata", Via della Ricerca Scientifica 1, I-00133, Roma (Italy). E-mail: larisa.lvova@uniroma2.it.

[c]Dipartimento di Scienze Pure e Applicate, Università degli Studi di Urbino "Carlo Bo", via della Stazione 4, I-61029 Urbino (Italy). E-mail: eleonora.macedi@uniurb.it.

[d]UK National Crystallography Service, School of Chemistry, Faculty of Engineering and Physical Sciences, University of Southampton, SO17 1BJ, Southampton (United Kingdom).

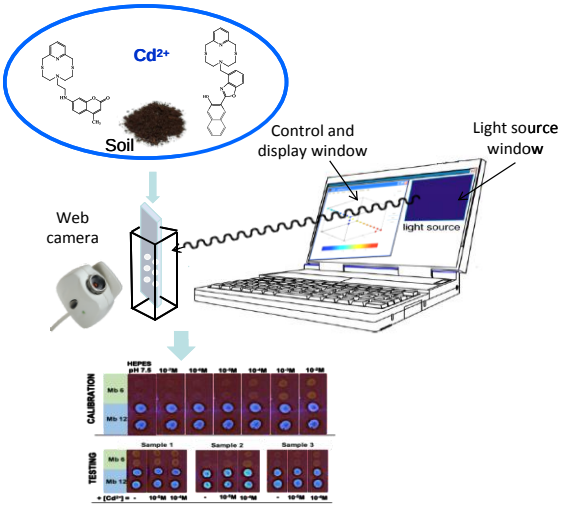

A fluorescent sensor array for the quantitative determination of Cd^{2+} in soils based on two N_2S_2 pyridinophane chemosensors is presented.

Authors biographies for

N_2S_2 Pyridinophane-Based Fluorescent Chemosensors for Selective Optical Detection of Cd^{2+} in Soils

Alessandra Garau,[a] Larisa Lvova,*[b] Eleonora Macedi,*[c] Gianluca Ambrosi,[c] M. Carla Aragoni,[a] Massimiliano Arca,[a] Claudia Caltagirone,[a] Simon J. Coles,[d] Mauro Formica,[c] Vieri Fusi,[c] Luca Giorgi,[c] Francesco Isaia,[a] Vito Lippolis,[a] James B. Orton [d] and Roberto Paolesse [c]*

[a]Dipartimento di Scienze Chimiche e Geologiche, Università degli Studi di Cagliari, S.S. 554 Bivio per Sestu, I-09042 Monserrato, Cagliari (Italy). E-mail: agarau@unica.it.

[b]Dipartimento di Scienze e Tecnologie Chimiche, Università di Roma "Tor Vergata", Via della Ricerca Scientifica 1, I-00133, Roma (Italy). E-mail: larisa.lvova@uniroma2.it.

[c]Dipartimento di Scienze Pure e Applicate, Università degli Studi di Urbino "Carlo Bo", via della Stazione 4, I-61029 Urbino (Italy). E-mail: eleonora.macedi@uniurb.it.

[d]UK National Crystallography Service, School of Chemistry, Faculty of Engineering and Physical Sciences, University of Southampton, SO17 1BJ, Southampton (United Kingdom).

Alessandra Garau graduated in Biological Science in 1991 at the University of Cagliari. In 1997 she received her PhD degree in Chemistry from the University of Cagliari, Italy. Since 2000 she is technician-researcher at the University of Cagliari. She has published 105 papers. Research interests include: Supramolecular Chemistry, design, synthesis and characterisation of chemosensors for cation and anion recognition, synthesis and coordination chemistry of macrocyclic ligands and fluorescent materials.

Publications:
https://www.scopus.com/authid/detail.uri?authorId=7004550328
https://orcid.org/0000-0001-5865-8137

Larisa Lvova received her M.S. (1996), Ph.D. (1999) degrees in Physical Chemistry and Dr.Sc. (2017) degree in Analytical Chemistry from St. Petersburg State University, Russia, and Ph.D. (2012) in Chemical Sciences from "Tor Vergata" University, Rome, Italy. Currently she is assistant professor at "Tor Vergata" University, Rome, Italy. L. Lvova does research in Electrochemistry, Analytical Chemistry, Chemometrics and Multisensor analysis. Her main research activity includes the design, synthesis and characterization of novel sensing materials for chemical sensors, both electrochemical and optical, and their applications. She is author of 62 publications in peer-reviewed journals and over 70 presentations in International meetings.

Publications:
https://www.scopus.com/authid/detail.uri?authorId=6603451079
https://orcid.org/0000-0002-1137-6973

Eleonora Macedi obtained her MSc degree in Pharmaceutical Chemistry and Technology in 2005 and Ph.D. in Chemical and Pharmaceutical Sciences in 2009 from University of Urbino, Italy. Currently she is a fixed term researcher at the Department of Pure and Applied Sciences of University of Urbino. Her current research interests are focused on the design, synthesis and characterization of linear and macrocyclic polyamine-based systems for the recognition and sensing of metal cations, anions and species of biological interest.

Publications:
https://www.scopus.com/authid/detail.uri?authorId=24462297500
https://orcid.org/0000-0003-0251-901X

Gianluca Ambrosi studied chemistry at University of Bologna, Italy, before taking his Ph.D. in 2006 in chemical and pharmaceutical sciences at the University of Urbino "Carlo Bo", Italy. Currently he is a laboratory technician at the University of Urbino "Carlo Bo", Italy. Gianluca Ambrosi's research interests focus on the supramolecular chemistry of polyamine receptors aiming to exploit these ligands for molecular recognition, detection and sensing of metal ions and anions of biological and environmental relevance. He is co-author of 40 publications in peer-reviewed journals.

Publications:
https://www.scopus.com/authid/detail.uri?authorId=7006385310

M. Carla Aragoni graduated *summa cum laude* in Chemistry in 1994 and received PhD in Chemical Science in 2000. She works at the University of Cagliari since 1997 as researcher in Inorganic Chemistry and since 2014 as Associate Professor. Her research interests mainly regard crystal engineering based on the design, synthesis and spectroscopic and structural characterization of supramolecular networks built up by coordination-, halogen- and hydrogen-bonds between polypyridyl-based spacers and different Lewis acids with applications as antitumoral and antimicrobic agents and luminescent based ion sensors. She is co-author of 110 publications in peer-reviewed journals and over 80 presentations in National and International Meetings.

Publications:
ORCID: http://orcid.org/0000-0002-5010-7370
WOS ID: AAG-1802-2019
Scopus Author: 6603722820

Massimiliano Arca received his degree in Chemistry in 1994 from the University of Cagliari, Italy, and a Ph.D. in Chemical Sciences in 1999 from the University of Sassari, Italy. Currently he is full professor of General and Inorganic Chemistry at the University of Cagliari, Italy. His research interests are focused on the experimental and theoretical investigation on chalcogen and pnicogen donors and their interactions with dihalogens/interhalogens, main group and transition metal ions, with applications spanning from NLO, photoconductivity, and sensors to medicinal chemistry and the restoration of cultural heritage. He is author of more than 160 publications in peer-reviewed journals and 100 presentations to International meetings.

Publications:
Scopus Author ID: 7006912042
Orcid ID: 0000-0002-0058-6406
WoS ResearcherID: S-4037-2019

Claudia Caltagirone got her master's degree (2001) and PhD in Chemistry (2006) in Cagliari under the supervision of Prof. Vito Lippolis. After the PhD she became Assistant Professor at the University of Cagliari and moved to UK for 2 years (2006-2008) as academic visitor in the group of Prof. Philip Gale. Since 2016 she is Associate Professor at the University of Cagliari, Italy. Her main research interests are the design, synthesis and characterisation of molecular chemosensors for anion and cation recognition, the development of novel self-assembling materials, the development of novel lipid-based nanoparticles for nanomedicine applications. She is author of 90 papers in peer reviewed journals .

Publications:
https://www.scopus.com/authid/detail.uri?authorId=8079729000
http://orcid.org/0000-0002-4302-0234

Simon Coles obtained his BSc and PhD in structural systematics and molecular modelling at the University of Wales, Cardiff in 1992 and 1997 respectively. He then moved to a PDRA appointment with the Royal Institution to build the highly successful Small Molecule Single Crystal beamline, 9.8, at the Daresbury synchrotron. In 1998 Simon moved to Southampton to establish a new laboratory and manage the National Crystallography Service. Simon transferred to Chemistry staff in July 2009, when he took over the role of Director of the National Crystallography Service and in 2019 he also became Director of the UK Physical Sciences Data-science Service. Simon is an author on over 900 papers covering the areas of structural chemistry, support for chemical synthesis and chemical information and is one of the world's most prolific chemical crystallographers.

Publications:
http://orcid.org/0000-0001-8414-9272)

Mauro Formica received his Degree in Chemistry (1991) from the University of Messina, Italy, and Ph.D. (2008) in Chemical Sciences from the University of Camerino, Italy. Currently he is associate professor at the University of Urbino "Carlo Bo", Italy. The research interests of M. Formica are focused on Coordination Chemistry, Supramolecolar Chemistry and Photochemistry. His main research activity includes the design, synthesis and characterization of photoactive ligands able to be used as chemosensor for metal ions, anions and biologic substrates. He is co-author of 75 publications in peer-reviewed journals, 2 patents and over 70 presentations in International meetings.

Publications:
https://www.scopus.com/authid/detail.uri?authorId=7006308385
https://orcid.org/0000-0002-2087-4624

Vieri Fusi received his Ph.D. in Chemical Sciences from University of Florence (Italy) in 1995 where he graduated in Chemistry in 1991. Actually, he is full professor of General and Inorganic Chemistry at the University of Urbino, Italy. The research of V. Fusi mainly lies in the Supramolecular Chemistry, Coordination Chemistry and Bioinorganic Chemistry fields. His activity principally regards the design and synthesis of new molecular systems, most of them having a macrocyclic skeleton, and the study of their metal complex-formation properties. In the last years, his interest was focused on the development of fluorescent chemosensors for multiple applications as well as on molecular and metal-systems with antineoplastic activity. He is author of 138 publications in peer-reviewed journals, four patents, 2 books.

Publications:
https://www.scopus.com/authid/detail.uri?authorId=7006296052
https://orcid.org/0000-0002-7627-8637

Luca Giorgi received his Degree in Chemistry (1996) from the University Bologna, Italy, and Ph.D. (2005) in Chemical Sciences from the University of Camerino, Italy. Currently he is associate professor at the University of Urbino "Carlo Bo", Italy. The research interests of L. Giorgi lie on Coordination Chemistry, Supramolecolar Chemistry and Photochmistry. His main research activity includes the design, synthesis and characterization of photoactive ligands able to be used as chemosensor for metal ions, anions and biologic substrates. He is co-author of 77 publications in peer-reviewed journals and two textbook of general chemistry.

Publications:
https://orcid.org/0000-0001-5734-2835

Francesco Isaia received his degree in Industrial Chemistry from the University of Cagliari. Currently he is assistant professor in General and Inorganic Chemistry at the University of Cagliari He has published 180 papers. Main research activity is on the synthesis and characterization of metal complexes of gold and palladium with thioamido-containing molecules.

Publications:
https://www.scopus.com/authid/detail.uri?authorId=7003598319
https://orcid.org/0000-0003-2139-8188

Vito Lippolis graduated in chemistry in 1991 at the University of Pisa, Italy, and in the same year gained a diploma in chemistry at the ‘‘Scuola Normale Superiore’’ of Pisa. In 2000 he received his PhD degree from the University of Nottingham, UK, under the supervision of Professor Martin Schröder. He has published about 300 publications. His research interests mainly include: coordination chemistry of macrocyclic ligands, development of molecular sensors and ionophores for heavy metal ions, and fluorescent materials.

Publications:
https://people.unica.it/vitolippolis/prodotti-della-ricerca/

James B. Orton obtained his Master's Degree in 2002 (under the supervision of Prof Geoffrey R. Luckhurst), and his PhD in 2006 (under the joint supervision of Dr Martin C. Grossel and Prof Michael B. Hursthouse). He then became a PDRA for Anthony K Cheetham until he left academia in 2008. Since 2017, James he has become part of the UK National Crystallography Service, Southampton (directed by Prof Simon J Coles). His main areas of interest are supramolecular assembly, crystal engendering, chiral metal-organic frameworks and crystal sponge materials.

Publications:
https://www.scopus.com/authid/detail.uri?authorId=8588795000
http://orcid.org/0000-0002-5362-6969

Roberto Paolesse is a full professor of general chemistry at the Department of Chemical Science and Technology of the University of Rome Tor Vergata. His research interests include the synthesis and reactivity of transition metal complexes with porphyrins and related macrocycles and the development and application of chemical sensors. Ha authored more than 300 papers on international journals and conferences. R. Paolesse was chairman of the 4th International Conference on Porphyrins and Phtalocyanines (Rome 2006), and serves in the Editorial Board of the Journal of Porphyrins and Phththalocyanines and in the steering committee of the International Meeting of Chemical Sensors conferences series.

Publications:
Scopus Author ID: 7007177639;
orcid.org/0000-0002-2380-1404

*Declaration of Interest Statement

Declaration of interests for

N_2S_2 Pyridinophane-Based Fluorescent Chemosensors for Selective Optical Detection of Cd^{2+} in Soils

Alessandra Garau,[a] Larisa Lvova,*[b] Eleonora Macedi,*[c] Gianluca Ambrosi,[c] M. Carla Aragoni,[a] Massimiliano Arca,[a] Claudia Caltagirone,[a] Simon J. Coles,[d] Mauro Formica,[c] Vieri Fusi,[c] Luca Giorgi,[c] Francesco Isaia,[a] Vito Lippolis,[a] James B. Orton [d] and Roberto Paolesse [c]*

[a]Dipartimento di Scienze Chimiche e Geologiche, Università degli Studi di Cagliari, S.S. 554 Bivio per Sestu, I-09042 Monserrato, Cagliari (Italy). E-mail: agarau@unica.it.

[b]Dipartimento di Scienze e Tecnologie Chimiche, Università di Roma "Tor Vergata", Via della Ricerca Scientifica 1, I-00133, Roma (Italy). E-mail: larisa.lvova@uniroma2.it.

[c]Dipartimento di Scienze Pure e Applicate, Università degli Studi di Urbino "Carlo Bo", via della Stazione 4, I-61029 Urbino (Italy). E-mail: eleonora.macedi@uniurb.it.

[d]UK National Crystallography Service, School of Chemistry, Faculty of Engineering and Physical Sciences, University of Southampton, SO17 1BJ, Southampton (United Kingdom).

☒ The authors declare that they have no known competing financial interests or personal relationships that could have appeared to influence the work reported in this paper.

Credit Author statement for

N_2S_2 Pyridinophane-Based Fluorescent Chemosensors for Selective Optical Detection of Cd^{2+} in Soils

Alessandra Garau,[a] Larisa Lvova,*[b] Eleonora Macedi,*[c] Gianluca Ambrosi,[c] M. Carla Aragoni,[a] Massimiliano Arca,[a] Claudia Caltagirone,[a] Simon J. Coles,[d] Mauro Formica,[c] Vieri Fusi,[c] Luca Giorgi,[c] Francesco Isaia,[a] Vito Lippolis,[a] James B. Orton [d] and Roberto Paolesse [c]*

[a]Dipartimento di Scienze Chimiche e Geologiche, Università degli Studi di Cagliari, S.S. 554 Bivio per Sestu, I-09042 Monserrato, Cagliari (Italy). E-mail: agarau@unica.it.

[b]Dipartimento di Scienze e Tecnologie Chimiche, Università di Roma "Tor Vergata", Via della Ricerca Scientifica 1, I-00133, Roma (Italy). E-mail: larisa.lvova@uniroma2.it.

[c]Dipartimento di Scienze Pure e Applicate, Università degli Studi di Urbino "Carlo Bo", via della Stazione 4, I-61029 Urbino (Italy). E-mail: eleonora.macedi@uniurb.it.

[d]UK National Crystallography Service, School of Chemistry, Faculty of Engineering and Physical Sciences, University of Southampton, SO17 1BJ, Southampton (United Kingdom).

- Synthesis and solution studies on **L1**: **Gianluca Ambrosi, Luca Giorgi, Eleonora Macedi**;
- ^{1}H- and ^{13}C NMR studies on **L1**: **Mauro Formica;**
- Synthesis and solution studies on **L2**: **Alessandra Garau, Claudia Caltagirone, M. Carla Aragoni**;
- ^{1}H- and ^{13}C NMR studies on **L2**: **Alessandra Garau, Francesco Isaia, Massimiliano Arca;**
- Development and study of polymeric membrane optodes: **Larisa Lvova, Roberto Paolesse;**
- Crystallographic studies: **James B. Orton, Simon J. Coles**;
- Supervision and writing of the manuscript: **Alessandra Garau, Larisa Lvova, Eleonora Macedi, Vieri Fusi, Vito Lippolis, Roberto Paolesse.**